



The Journey to Dental-Dedicated Magnetic Resonance Imaging

Strategic
Partner

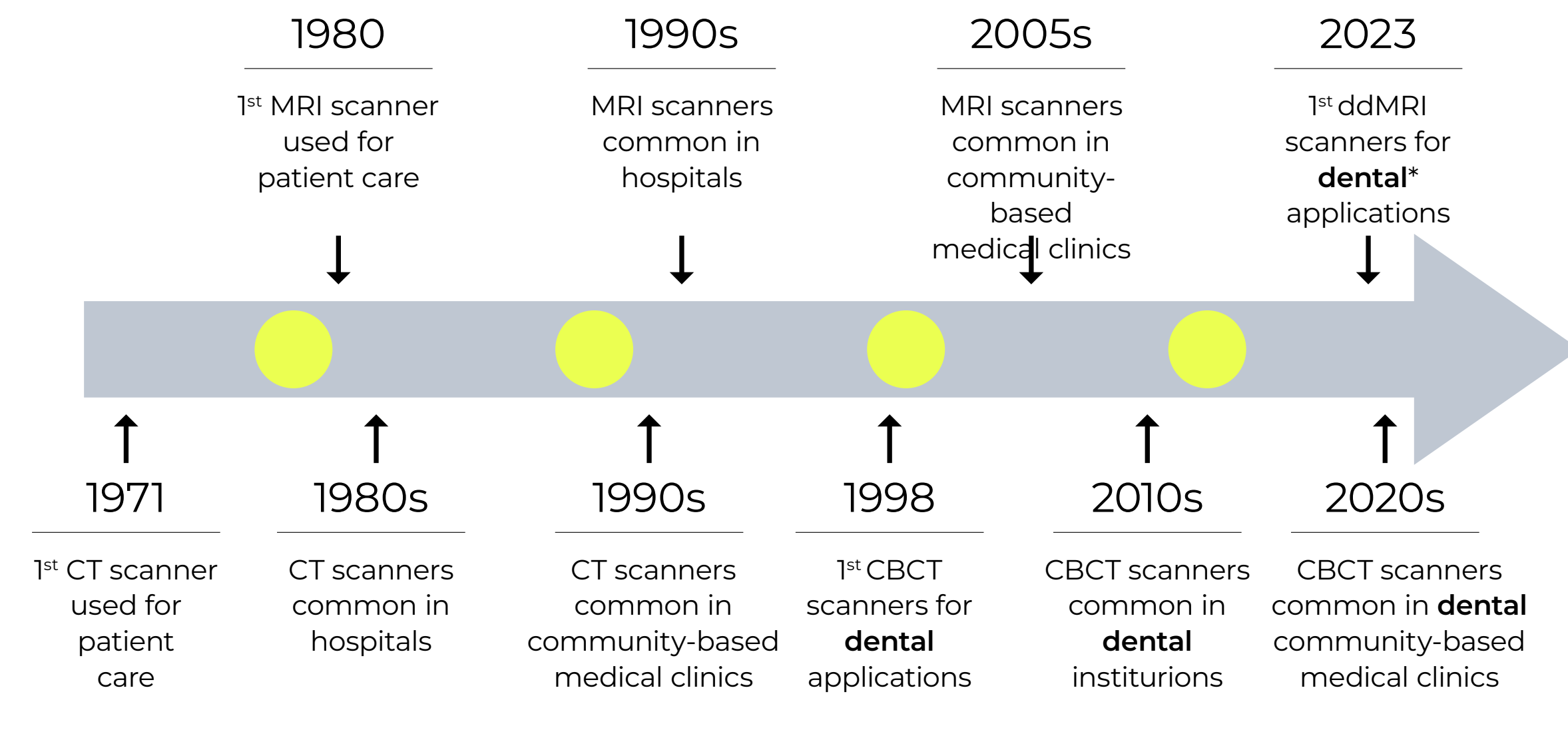


Imaging in dentistry: the parallel with radiology

This whitepaper aims to give further information on how the dental-dedicated MRI (ddMRI) works, what it can bring to dentistry that existing techniques do not already provide, and the introduction of the the first case studies, highlighting initial applications where ddMRI can be beneficial in dental medicine.

The introduction of medical imaging into healthcare system redefined the way diagnostics and treatment monitoring were done. Hospitals no longer had to host patients for an extended post-procedure recovery time, and more significantly the diagnosis could be done earlier, which meant more effective treatment and preventive measures could be planned in a timely fashion.

Dentistry first used diagnostic imaging in 1896, starting within months of Roentgen's discovery of "x-rays".¹ Since then, the profession has continually evolved to incorporate additional imaging modalities into practice, such as panoramic radiographs, digital imaging, and cone-beam computed tomography.^{1,2,3} With every subsequent modality, novel features have emerged, enlightening clinicians in new ways, that improved patient care. The next technological breakthrough to enhance patient care has been reached with the introduction of ddMRI.*



Technological developments over time improve image quality, expand use applications, and reduce barriers for widespread adoption

Fig. 1: Timeline depicting the evolution of 3D imaging modalities in healthcare

Like medicine, dentistry has greatly benefited from the introduction of CT into the existing clinical practice model (i.e., cone-beam CT, CBCT). And like medicine, dentistry will greatly benefit from the introduction of MRI into the existing clinical practice model (i.e., ddMRI).

* First ddMRI scanners for validating dental applications.

1 Pauwels R. History of dental radiology: evolution of 2D and 3D imaging modalities. Medical Physics International Journal. 2020;3:235-77.
 2 Hallikainen D. History of panoramic radiography. Acta Radiol. 1996;37(3 Pt 2):441-5. Epub 1996/05/01. doi:10.1177/02841851960373P207. PubMed PMID: 8652310.
 3 Kiljunen T, Kaasalainen T, Suomalainen A, Korttinen M. Dental cone beam CT: A review. Phys Med. 2015;31(8):844-60. Epub 2015/10/21. doi:10.1016/j.ejmp.2015.09.004. PubMed PMID: 26481816.



Why to think about MRI in dentistry?

The further development of MRI for dentistry has been expected as the technological advancements in imaging progress. MRI has, ever since it was initially developed in 1980, continuously developed in a way that mirrors the development trends observed for computed tomography (CT) imaging, but with a decade of lag time (Fig. 1). We are now at a point where MRI has been widely adopted in medical practice, and we are expecting to see the same progress, starting in dental universities, for oral diagnostics over time. Up until now, conventional MRI systems have been difficult to fit into dentistry. There have been several barriers that we had to overcome to reach this point.

Advances in hardware and software technologies have simplified the integration of MRI into new environments that had conventionally only the capacity to offer X-ray and CT imaging services. As compared to conventional MRI systems, a new breed of light-weight magnet technology enables the cooling of the superconducting magnet with less than a liter of helium, removing the need for extensive infrastructure adaptation such as constructing a quench pipe. The built-in automation in such a technology, not only facilitates automated reaction to unpredictable power or temperature conditions, but also enables the different aspects of operation from patient setup to scanning with limited on-site expertise. Furthermore, the design elements in this new technology, which focus on patient experience, enable the inclusion of new patient groups that have previously been excluded, as well as the advent of new clinical applications that have conventionally been routed to CT or X-ray systems. These key characteristics create a promising outlook for the widespread availability of MRI systems in similar fashion as X-ray and CT.

With the knowledge that is currently known about the advantages of MRI in radiology, there are also benefits for oral diagnostics and non-ionizing radiation-based imaging⁴ in children conceivable with the use of MRI technology, by making MRI technology also accessible in the dental space.

Dentsply Sirona and Siemens Healthineers have joined forces to facilitate the scientific introduction of MRI into dentistry. Through this scientific partnership, the companies work with leading global dental institutions to shine light on the advantages of MRI in preventive oral care and help transform the current state of corrective oral care delivery to include treatment planning and truly preventive care by bringing into light biological events and changes that were previously invisible to the naked eye or existing imaging modalities.

In the following sections, we present MRI technology in a nutshell, the current state-of-the-art MRI technology for dentistry, and its clinical validation, provided by our clinical partners. Highlighting how some of the unique engineering features of a new breed of MRI systems can break down the barriers of dental access to MRI and facilitate the integration of this imaging modality into dentistry.



Magnetic Resonance in a nutshell

X-ray and CBCT imaging are both established imaging modalities in dentistry. X-ray imaging is ideally suited to provide information about alignment, roots, and overall health. CBCT is used in more advanced treatments such as implant planning and post-implant alignment assessment. In all these use-cases x-ray attenuation of the relevant anatomical hard-tissue structures provides sufficient information. MRI, as a technology, works in an entirely different way and – by it's different nature – is able to provide complementary soft tissue contrast. To gain an appreciation for the uniqueness of MRI, both from the angle of opportunities and considerations, one has to start by understanding the requirements for a successful MRI installation and operation. Let's start by talking about how MRI works.

How the MR images are made

MRI utilizes the intrinsic abundance of water molecule in the body to generate images of underlying tissue and pathology. Various tissues inside the body consist of different water content and the different parts of the same tissue, due to pathology for instance, can also contain varying water content. This enables an MRI scanner to generate images with exquisite soft tissue contrast – images that enable the effective differentiation of slightest change in the health of underlying tissue. In doing so, MRI makes simultaneous use of three different magnetic fields to move the unpaired protons in the water molecule (here forth referred to as 'spins') in a predictable way. The detection of the signal resulting from the return of these spins to their equilibrium position results in a 3D representation of the underlying tissue. Here is how each magnetic field contributes to the image generation:

The main magnetic field

The primary magnetic field that MRI uses to control the unpaired protons in the patient's body is the main magnetic field (Fig. 2), which is often used to quantify the strength of the MRI system (e.g., 1.5T, 7T magnets – T, or Tesla, is the SI unit for magnetic field). This field is the strongest magnetic field in the MRI system architecture and is one that is always on and always at one single value – from the time of installation to the time when the system is uninstalled and removed. This field is also the main reason behind many safety measures put in place during the siting of an MRI system.

The large magnetic field is created using a high current that runs through special coil material. This level of current would normally result in significant amount of heating, which would make the system inefficient. However, in an MRI system, using liquid helium the coils can be cooled to a point of virtually zero resistance, which means the large current can flow seamlessly, which in turn means the magnetic field can be maintained for the lifetime of the system. A conventional magnet design can require up to 1500 liters of liquid helium.

Once a subject is placed inside the magnetic field of an MRI system the spins are forced to align with the orientation of the field. This gives the MRI system a predictable starting point.

The gradient field

Spatial localization of the different parts of the body is taken care of by the gradient fields (Fig. 2). These fields generate very small deviations from the main magnetic field that inform the receiving antennas where, spatially, the information they receive come from. Whereas the main magnetic field (in a clinical setting) is typically in order of single digit Tesla, the gradient fields are often in order of mT per meter.

The radiofrequency fields

The last field that completes the hardware requirement for an MRI system is the radiofrequency (RF) field (Fig. 2). The role that this component plays is to, in a predictable fashion, choreograph the movement of the spins inside the body – this gives rise to the unique contrast mechanisms. In simple terms, the deposition of the RF energy, as a result of this field will lead to a predictable motion in the underlying spins away from the direction of the main field, and as soon as this field is removed, the energy that is absorbed gets released as the spins return to their steady state (i.e., their initial alignment with the main magnetic field, which, as said, is the only field that remains in effect at all times). This emitted energy is picked up by RF antennas, referred to, in the MRI universe, as receiver coils in Fig. 2. From here, the software programs take the data and transform them into a 2D or 3D image, much like the CT algorithms do.

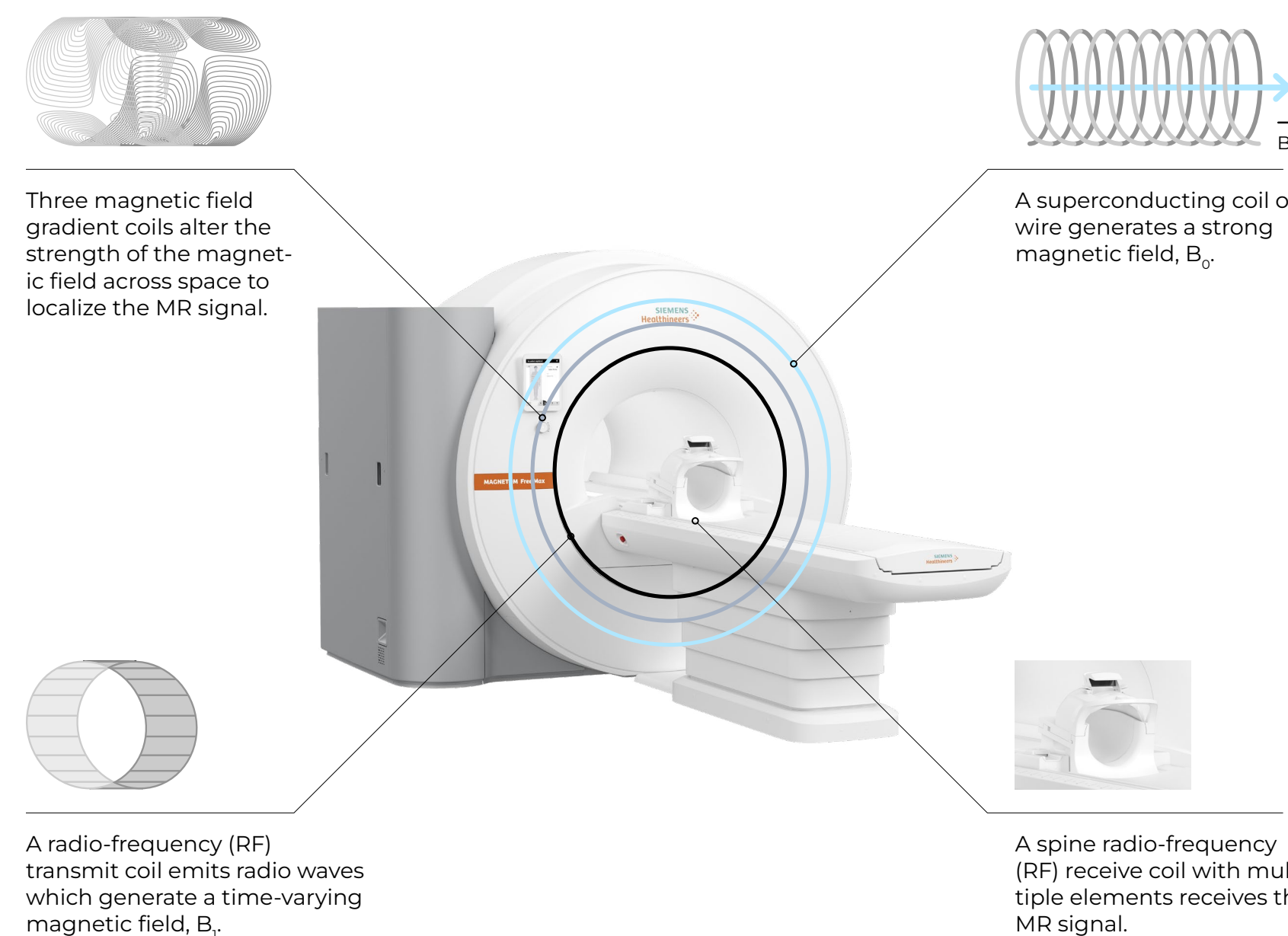


Fig. 2: Basic components of an MRI machine



Common MRI sequences

In MRI literature, one often comes across terms such as ‘proton density (PD)-weighting’, ‘T1-weighting’, or ‘T2-weighting’. These terms refer to the specific contrast mechanisms in an MR image.

Proton density (PD)-weighting

PD-weighted contrast reflects contrast produced predominantly by the intrinsic water content differences in the tissues – for example the tissue with high mineral content, such as teeth, have lower water content and fewer spins to give rise to MRI signal, while muscles, gums, and many pathologies such as edema are high on water content and therefore give rise to high levels of MRI signal.

T1-weighting

T1-weighted contrast arises from the varying characteristics of the different tissues in how long their respective spin groups take to realign with the main magnetic field after the RF field is removed; T1 is the time constant that reflects this characteristic. A tissue with low water content (e.g., teeth and bone) has a small T1 time constant and therefore appears darker on a T1-weighted image. Remember, after the RF field is turned off, it is a race towards equilibrium for the spins in the different tissues and no two tissues display the same contrast on these images.

T2-weighting

T2-weighted contrast arises from the varying characteristics of the different tissue in how long it takes for their respective spin groups to stop emitting the signal that was being generated while the RF field was active; T2 signifies the time required for this signal to decay away.

A chart depicting the expected tissue contrast in each of the above mentioned contrast mechanisms is shown in Fig. 3. These are some of the key contrast sub-types achievable with an MRI system. In the radiology world, many more contrasts have been proposed and explored, but those topics are not in the scope of this whitepaper – this, however, clearly delineates the strength of MRI, which is in its ability to achieve soft tissue contrast in ways no other imaging modality can match!

	 High Signal Intensity	 Intermediate Signal Intensity	 Low Signal Intensity	 Undetectable Signal Intensity
T1 weighted sequence	fat (bone marrow)	dental pulp, dental abscess/ inflammation	nerves, ligaments, muscles, cysts, mucous membranes, salivary glands	enamel, dentin, cortical bone, air
T2 weighted sequence	dental abscess/inflammation, fat (bone marrow), cysts	dental pulp, mucous membranes, salivary glands	nerves, ligaments, muscles	enamel, dentin, cortical bone, TMJ disc, air
Proton Density	dental abscess/inflammation, fat (bone marrow)	dental pulp, cysts, mucous membranes, salivary glands	nerves, ligaments, muscles	enamel, dentin, cortical bone, TMJ disc, air

Fig. 3: Tissue appearances in MRI based on common sequences*

* Note: Formal studies to definitively determine tissue types and appearances are still pending. This table is preliminary and based on medical literature and limited dental experience.



Requirements for MRI installation and operation

Successful installation of a conventional MRI system requires a series of infrastructure adaptations. Importantly, several safety measures must be put in place:

The system needs to be placed in a secure environment where the floor can tolerate the weight of the magnet. The good news is, the new generation of MRI scanners have a considerably lower weight, as well as overall dimension – this makes them far easier to site on upper floors, when needed, and brought into the final installation zone with minimal to no infrastructure adaptation.

The room where the scanner will be sitting has to also be shielded to protect the public against the large magnetic field of the system as well as to prevent any incoming disruptive signal in the same frequency range of the operation of the magnet. This ensures good images are generated during each examination. The advantage of having a dedicated field strength for a ddMRI system is that an ideal balance between safety and various other factors, such as the ability to image in presence of dental and mandible implants, can be met.

Another important safety measure that needs to be put in place is the construction of a quench pipe – this is a ‘chimney’ that allows for an exit pathway for the helium that’s used to cool down the system hardware. Fortunately, the new breed of MRI systems, MAGNETOM Free.Max, requires a mere 0.7l helium, which is sealed for life in such a way that it doesn’t leave the system under any circumstance. This means no major infrastructure adaptation is needed and the safety requirements are still met, by design!

On the operation side, MRI is a sophisticated imaging modality that requires careful optimization of several imaging parameters. A change to any one imaging parameter can result in suboptimal image quality or a change in image contrast, which can potentially be misinterpreted. Successful operation of an MRI system requires an experienced user, which further limits the installation possibilities for MRI to locations where expertise for operating such a complex imaging modality is available. The new generation of MRI systems leverages artificial intelligence to enable patient workflow, providing a simplified user interface and requiring minimal user interaction with the system or the protocols. A similar setup, where user interaction with the system is optimized for dentistry significantly facilitates the adaption of MRI into this field.



Realization of ddMRI

So what is ddMRI? Simply, ddMRI is the tailoring of the hardware, software, and workflows specifically designed for acquisition in a dental clinic setting for dental indications. The culmination of tailoring all aspects of MR imaging brings forth new capabilities to address unmet clinical needs of dentistry. Compared to conventional MRI, ddMRI has a greatly reduced space requirement, offers shorter scan times (~3 minutes and less), greatly reduces artifacts from dental materials, and offers a simplified workflow which allows delegation of scanning to existing dental staff. In more detail, what this specifically means is:

- 1** Hardware components such as radiofrequency coils, gradient coils, and the main magnet itself have been made to meet the needs of a dental practice. A ddMRI should integrate a dedicated coil that allows for easy patient setup while ensuring excellent image acquisition.
- 2** Software components such as pulse sequences have been optimized for contrasts to highlight dental pathologies and craniofacial structures, to have greater resolution, focused fields of view, and orientation of imaging tailored to anatomy of interest for dentistry.
- 3** Dental-dedicated protocols: MR imaging offers the great advantage of depicting different tissues with different contrast by selectively manipulating the behavior of water molecules inside various tissues. A ddMRI should include specific protocols that can be simply executed without, or with minimal, operator interaction, similar to the extent of interaction in current dental X-ray and CBCT systems.
- 4** Workflows have been developed to simplify MRI acquisition via development of preselected pulse sequences based on dental indications, automated localization functionality, in-the-room set-up, scan times, and clean-up of 20 minutes or less, presentation of images in a dental-centric manner, image compatibility with existing software for seamless integration into the dental universities.
- 5** Dental-dedicated user interface and viewing: MR images, as used for diagnostics in radiology, have vastly different views compared to those that are used in dentistry. A ddMRI must include a user interface that is simplified and intelligent in such a way that all the required acquisition views are known to the system and executed in the background. The viewing software used to output the results of the examination should display the images in the conventional dental views. In addition, much like X-ray and CBCT, the images generated by MRI need to display only the dental-relevant information (i.e., no tissue outside of the oral cavity can be captured).

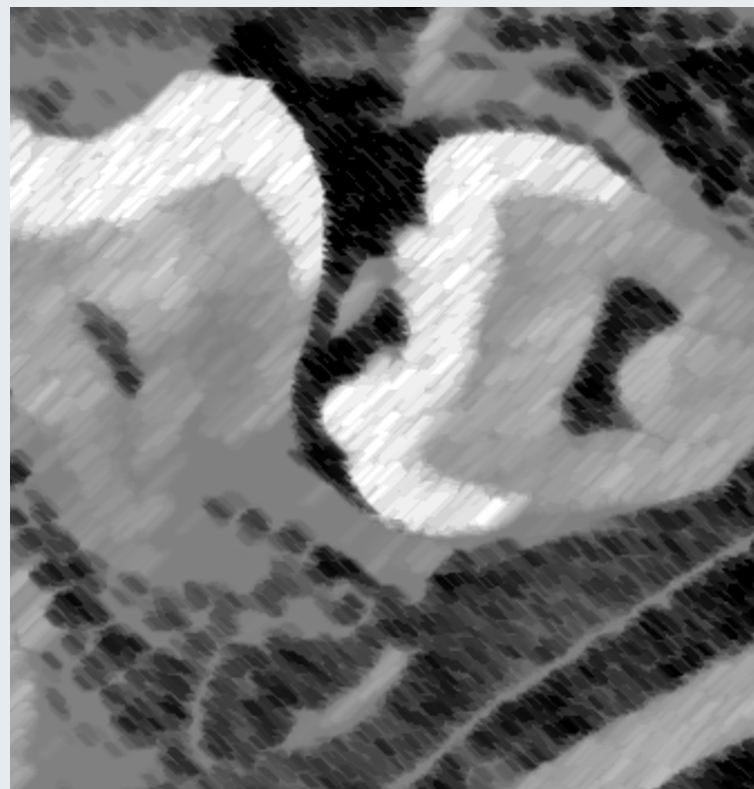
As with prior imaging modalities in dentistry that allowed new structures to be seen, ddMRI will now allow clinicians to visualize both hard and soft tissue structures simultaneously in 3D from the convenience of their own clinics.

Additionally, MRI does not expose patients to ionizing radiation¹, thus making it an ideal candidate for instances such as preventative screenings, serial monitoring of disease progression, imaging of children, and many more. Although some of this may sound complicated, it is important to remember that for ddMRI, user interactions are optimized for dentistry. This means that dentists and staff will not need to understand the physics to operate the units. They will have a workflow similar to that used with the complementary technology, like CBCT.

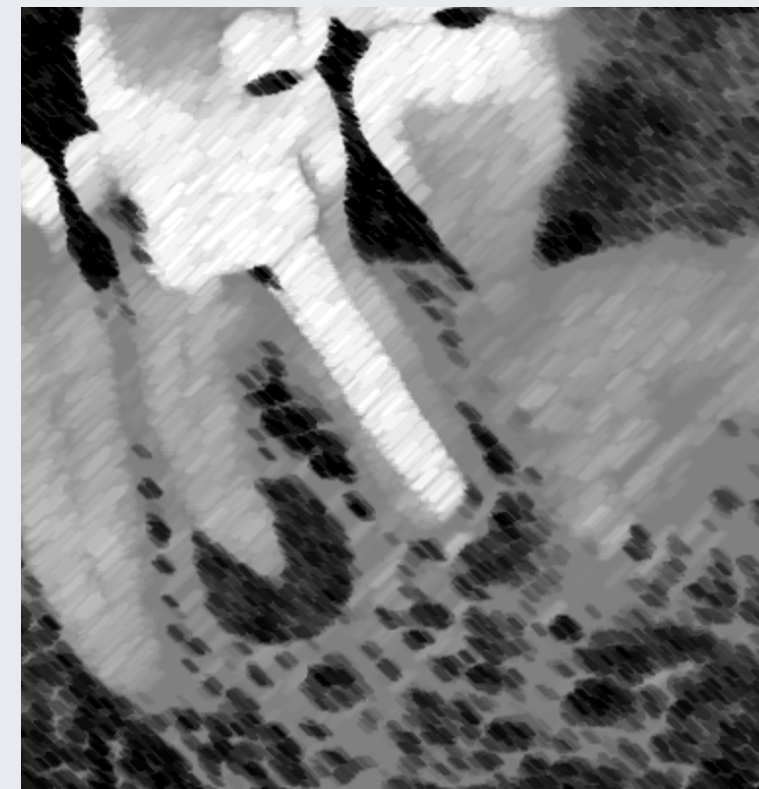
The following chapter presents first clinical cases that clearly depict the role that ddMRI could play in oral diagnostics in the future.

Clinical feasibility: case reports

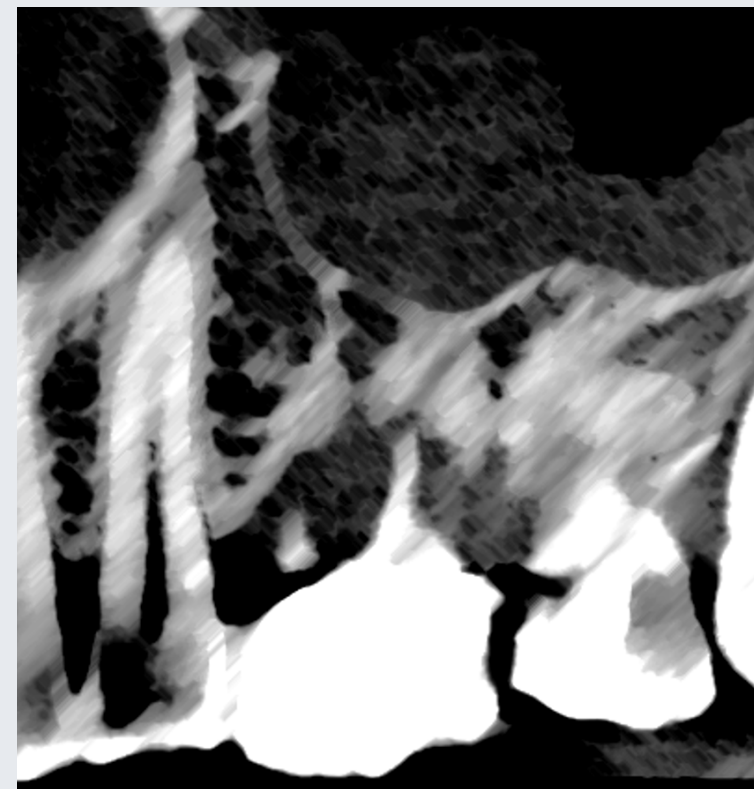
ddMRI is currently being used in non-inferiority clinical trials exploring diverse diagnostic tasks relevant to dentistry that include:

**1**

Providing diagnostic information related to extraction of lower third molars

**2**

Detecting the presence of apical periodontitis

**3**

Quantifying bone levels around teeth

**4**

Providing cephalometric and airway analysis in orthodontic patients

**5**

Assessing the anatomy of the temporomandibular joints

We present initial cases in which ddMRI has been explored. When clinically indicated, based on current imaging guidelines, we also provide panoramic and/or CBCT imaging in addition to ddMRI images for comparison. The images were acquired with the same dedicated system (scanner and dental coil) described in this document's coming chapters.

Lower third molars

The radiographic examination of mandibular third molars must provide information about the tooth, the surrounding bone, the neighbouring tooth and related anatomical structures. When planning the extraction of mandibular third molars, the key parameters to be observed are: (1) the anatomy and shape of the tooth and its roots; (2) the placement of the tooth in the mandible and its relationship with the mandibular canal (and the inferior alveolar nerve); (3) possible interactions with the mandibular second molars, such as the presence of significant bone loss between the second and the third molars, and the presence of external root resorption in the second molar caused by the third molar.^{1,2}

The current guidelines suggest that the transition from 2D (i.e., panoramic) to 3D (i.e., CBCT) imaging for the extraction of mandibular third molars should consider the amount of additional information needed and how this information will change the way the patient is to be treated. CBCT should only be used when the dentist has a particular clinical question that conventional imaging cannot answer in an individual patient case.³ For example, if the dentist is to opt between tooth extraction versus

coronectomy, or if the treatment plan should also include the treatment of possible root resorption in the lower second molar.

In the following case, provided by Associate Professor Rubens Spin-Neto and co-workers, from Aarhus University, the patient (a 21-year-old male) presented to the clinic already having a panoramic image taken and with a request for a CBCT to assist in defining the proper treatment plan regarding the right mandibular third molar. The panoramic image (Fig. 4) shows an intimate relationship between the fused roots and the mandibular canal with suspected fusion. It also indicates apparent bone loss along the distal aspect of the second molar, raising suspicion of external root resorption of that same tooth. The CBCT (Fig. 5) confirms both findings of the suspicions raised by the panoramic image and clearly shows no bony separation between the roots of the lower third molar and the mandibular canal.

In the ddMRI (Fig. 6), the exam session was defined to include a scout-image acquisition, followed by three separate PD-TSE slabs covering the sagittal, coronal, and axial planes of the mandibular third molar. The scout

acquisition took approximately 1 minute, and each plane of the PD-TSE was acquired in 2 minutes and 38 seconds. Considering patient preparation, placement and scanning, and clean-up, the total examination time was approximately 15 minutes.

Findings from the ddMRI were aligned with those of the CBCT, and all relevant anatomic components could be clearly depicted (canal fusion and 2nd molar resorption). Additionally, ddMRI added the possibility of observing the relevant soft tissue components in this case. The CBCT and ddMRI show that the lingual cortical bone wall is extremely thin, close to the root apex. The lingual nerve typically runs near this bony wall. Due to the wall's thinness, there is potential for the lingual plate to be fractured during the surgical procedure to extract the tooth, with possible subsequent injury to the nerve. However, based on ddMRI, it was possible to rule out any intimate proximity of the lingual nerve with that part of the lingual cortical bone, thus improving the surgeon's knowledge of the area and allowing the opportunity for improved informed consent.



Fig. 4: Panoramic image showing the intimate relation between the roots of the mandibular third molar and the mandibular canal. The image suggests bone loss along the distal face of the second molar and leads to the suspicion of external root resorption in the second molar.

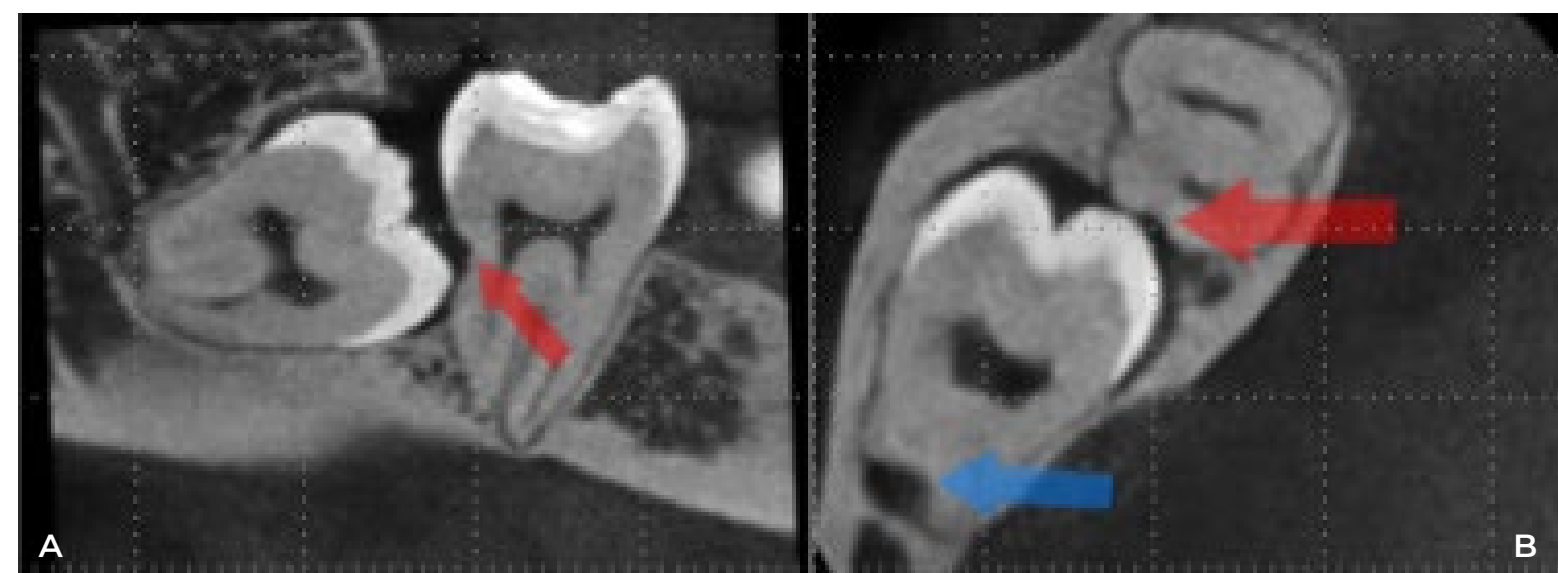


Fig. 5: CBCT of the same region, in which a bone loss exceeding 50% of the distal root length is also visible (A, red arrow). The image confirms the intimate relation between the roots and the mandibular canal and the absence of bony separation between the root and the canal (B, blue arrow). In addition, external yet mild root resorption in the second molar is confirmed (B, red arrow).

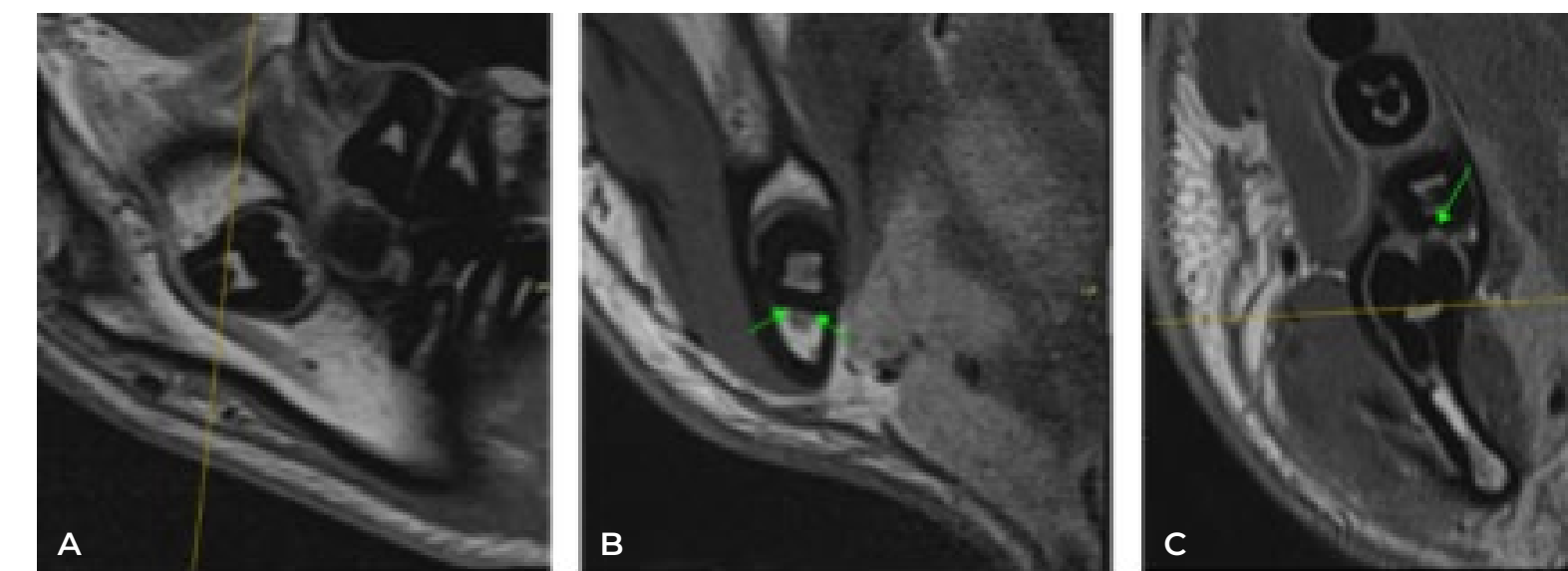


Fig. 6: ddMRI of the right mandibular third molar, confirming the intimate relation between the roots and the mandibular canal (A) and the absence of bony separation between the root and the canal (B, green arrows). The mild external root resorption in the second molar is also visible (C, green arrow). The yellow lines visible in A (sagittal plane) and C (axial plane) highlight the coronal plane presented in B.

1 Matzen LH, Wenzel A. Efficacy of CBCT for assessment of impacted mandibular third molars: a review – based on a hierarchical model of evidence. *Dentomaxillofac Radiol.* 2015;44(1):20140189. doi: 10.1259/dmfr.20140189.

2 Matzen LH, Schropp L, Spin-Neto R, Wenzel A. Use of cone beam computed tomography to assess significant imaging findings related to mandibular third molar impaction. *Oral Surg Oral Med Oral Pathol Oral Radiol.* 2017 Nov;124(5):506-516. doi: 10.1016/j.oooo.2017.07.007.

3 Matzen LH, Berkhout E. Cone beam CT imaging of the mandibular third molar: a position paper prepared by the European Academy of DentoMaxilloFacial Radiology (EADMFR). *Dentomaxillofac Radiol.* 2019 Jul;48(5):20190039. doi: 10.1259/dmfr.20190039.

Periapical structures

Endodontics demands radiographic imaging for diagnosis, treatment planning, therapy, and follow-up.¹ Bi- and three-dimensional radiographic information allows for identifying the anatomic structures inside (e.g., pulp chamber and canals) and outside (e.g., the periapical tissues) that cannot be visualised by clinical inspection. Furthermore, radiographic information is required to support clinical information during the diagnosis of pathologic alterations in those tissues, the most relevant being apical periodontitis (AP).² Besides the mere presence/absence of AP, the diagnosis in endodontics also includes the visualisation of other alterations, such as root fractures, internal and external root resorptions, and complex canal anatomy.²

The relationship between the radiographic appearance in periapical radiographs (PAs) and CBCT images and the histopathological state of the periapical bone is well-established.³ However, none of the currently used radiographic modalities can be considered as a reference standard for AP detection, and even technically perfect images may lead to false-positive and false-negative results. This is because PAs and CBCT images can only reveal mineralised (i.e., hard) tissues and cannot visualise

soft tissue processes associated with water retention within the bone, including inflammatory changes.⁴ However, endodontic disease occurs both in the soft- (i.e., the pulp) and hard-tissues, with earlier signs of disease beginning in the soft-tissues, prior to the patient presenting with the osseous destruction frequently detected today. Therefore, the lack of soft-tissue visualisation is one of the significant drawbacks of endodontic images. Furthermore, the ultimate piece of information about a tooth, its vitality status, is not yet available in any ionising-radiation-based imaging modality.

In the following case, provided by Associate Professor Rubens Spin-Neto and co-workers, from Aarhus University, the patient (a 41-year-old female) presented to the clinics with a request for a CBCT to assist in defining the proper diagnosis and treatment plan regarding the left maxillary central incisor. The dentist wanted to assess the extension of the external root resorption caused by orthodontic treatment and the possible presence of AP. Clinical tooth vitality tests and changes the colour of the tooth suggested the pulp was necrotised. The CBCT (Fig. 7) shows the presence of a well-defined apical radiolucency, allied with a

considerable alteration of the tooth apex due to resorption, and marked narrowing of the root canal, probably due to secondary calcification.

In the ddMRI (Fig. 8), the exam session was defined to include a scout-image acquisition, followed by two separate PD-TSE slabs, covering the sagittal and the coronal planes of the anterior maxillary region. The scout acquisition took approximately 1 minute, and each plane of the PD-TSE was acquired in 2 minutes and thirty-eight seconds. To allow a better understanding of the disease status in the periapical region, sagittal and coronal PD-TSE-STIR slabs were also acquired, each acquired in approximately 3 minutes. The examination time was approximately 21 minutes, considering the patient management time. The findings in the ddMRI agreed with those of the CBCT. ddMRI added relevant information about tooth vitality since the absence of hyperintense signal in the canal suggests that the pulp is necrotised. Also, the images suggest the absence of active inflammation in the periapical area, due to the signal intensities observed in the images acquired with and without STIR.



Fig. 7: CBCT of the left anterior incisor region, showing the presence of a well-defined apical radiolucency (red arrows on A and B), allied with a considerable alteration of the tooth apex due to external resorption (B, blue arrow).

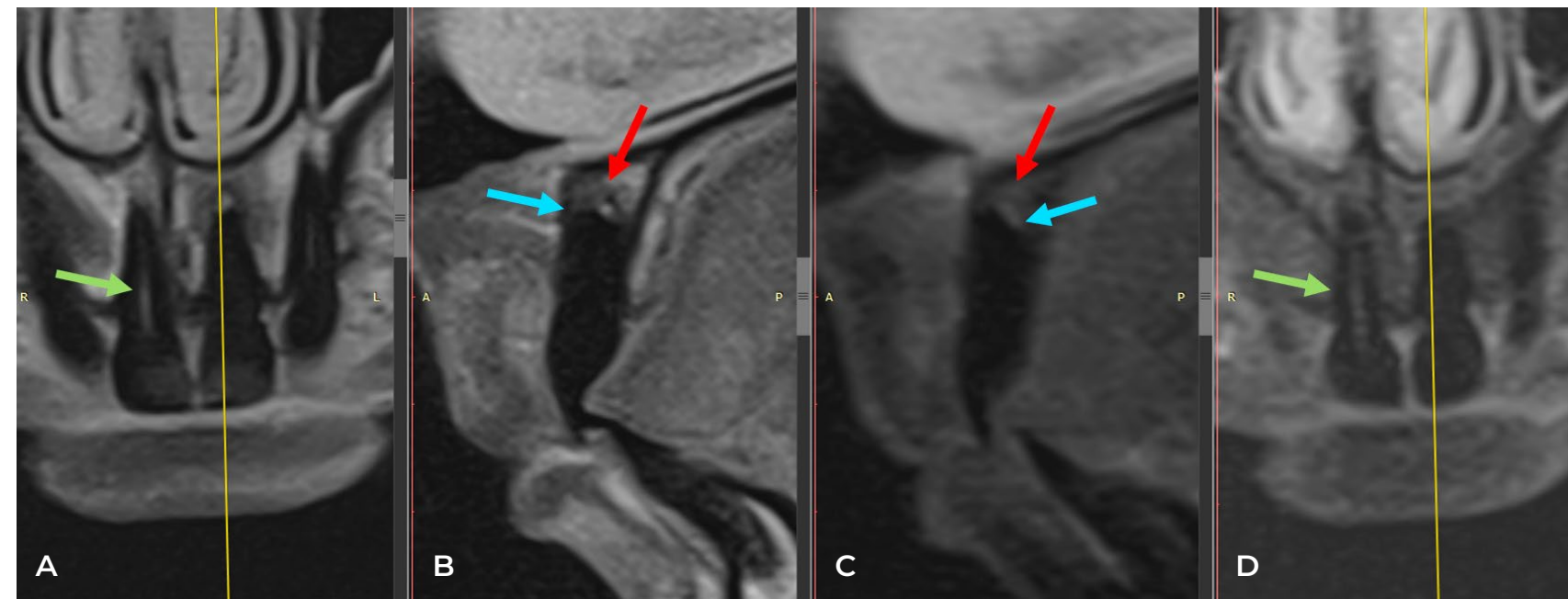


Fig. 8: ddMRI of the anterior maxillary region, confirming the presence of external root resorption of the left anterior incisor (B and C, blue arrows). The tooth is necrotised, as suggested by the absence of hyperintense signal in the canal, contrary to what is seen on the right central incisor (green arrows, PD-TSE on A, PD-TSE-STIR on D). The images also suggest the absence of active inflammation in the periapical area, due to the signal intensities observed in the images acquired with and without STIR (red arrows on B and C).

1 Setzer FC, Lee SM. Radiology in Endodontics. Dent Clin North Am. 2021 Jul;65(3):475-486. doi: 10.1016/j.cden.2021.02.004.

2 Patel S, Brown J, Semper J, Semper M, Abella F, Mannocci F. European Society of Endodontology (ESE) position statement: Use of cone beam computed tomography in Endodontics: developed by. Int Endod J 52(12): 1675-1678 (2019). doi: 10.1111/iej.13187.

3 Kruse C, Spin-Neto R, Wenzel A, Kirkevang LL. Cone beam computed tomography and periapical lesions: a systematic review analysing studies on diagnostic efficacy by a hierarchical model. Int Endod J. 2015 Sep;48(9):815-28. doi: 10.1111/iej.12388.

4 Probst M, Burian E, Robl T, Weidlich D, Karampinos D, Brunner T, Zimmer C, Probst FA, Folwaczny M.

Periapical structures

In the next case, provided by Associate Professor Rubens Spin-Neto and co-workers, from Aarhus University, the patient (a 43-year-old male) presented to the clinics with a request for a CBCT to investigate persistent symptoms following endodontic treatment performed more than five years before, in the left mandibular first molar. The CBCT (Fig. 9) shows the root-canal-treated tooth, with the presence of a well-defined apical radiolucency in the mesial root. The apex of the distal root presents signs of bone remodelling (i.e., healing).

In the ddMRI (Fig. 10 and Fig. 11), the exam session was defined to include a scout-image acquisition, followed by two separate PD-TSE slabs, covering the sagittal and the coronal planes of the anterior maxillary region. The scout acquisition took approximately 1 minute, and each plane of the PD-TSE was acquired in 2 minutes and thirty-eight seconds. To allow a better understanding of the disease status in the periapical region, sagittal and coronal PD-TSE-STIR slabs were also acquired, each acquired in approximately 3 minutes. Finally, to highlight the area with active disease, a T1-VIBE sequence was used, only in the sagittal plane (acquisition time of 3 minutes). The examination time was approximately 20 minutes, considering patient management time. The findings in the ddMRI agreed with those of the CBCT, highlighting the fact that ddMRI added relevant information about disease status. The images suggest the presence of active inflammation in the periapical area, due to the signal hyperintensity observed in the STIR and VIBE images.

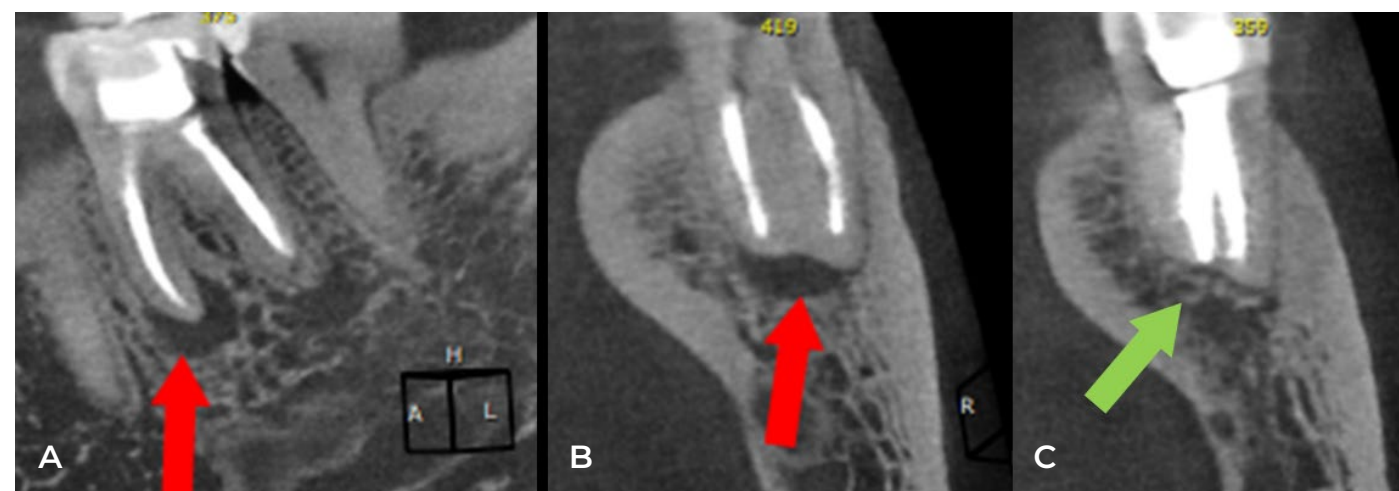


Fig. 9: CBCT of the left mandibular first molar. A well-defined apical radiolucency is seen in the mesial root (red arrows in A and B). The apex of the distal root presents signs of bone remodelling (green arrow in C).

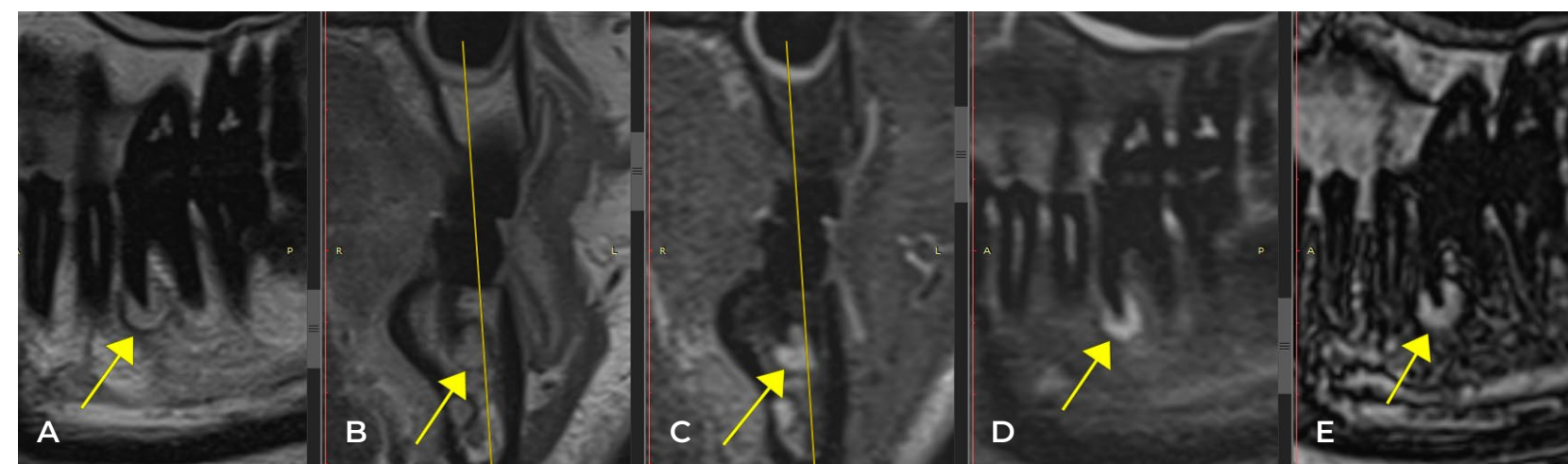


Fig. 10: ddMRI of the left mandibular first molar, confirming the presence of apical periodontitis (yellow arrows) in the mesial root. No artefacts due to the gutta percha used for endodontic treatment are seen in the images. A and B, PD-TSE images on the sagittal and coronal planes, respectively. C and D, PD-TSE-STIR images of the coronal and sagittal planes, respectively. E, T1-VIBE image of the sagittal plane.

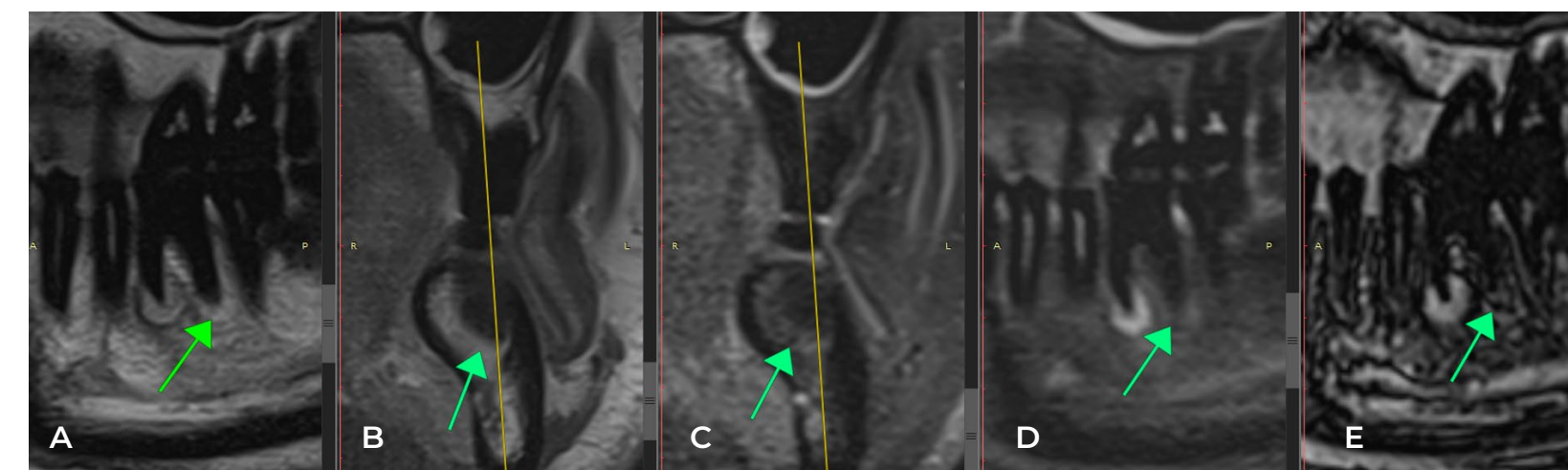


Fig. 11: ddMRI of the lower left first molar, confirming the presence of periapical healing (green arrows) in the distal root. No artefacts due to the gutta percha used for endodontic treatment are seen in the images. A and B, PD-TSE images on the sagittal and coronal planes, respectively. C and D, PD-TSE-STIR images of the coronal and sagittal planes, respectively. E, T1-VIBE image of the sagittal plane.

Periodontal structures

The inflammatory process that leads to periodontal disease starts in the gingival soft tissues and evolves to compromise the tooth-supporting tissues (e.g., the alveolar bone and the periodontal ligament)¹, leading to the resorption and breakdown of the periodontal tissue apparatus. Complementary to an increased probing depth measured clinically, radiographic images are often used to determine and visualise the altered marginal bone levels in the diagnosis of periodontitis and its stability for monitoring treatment outcomes.² CBCT additionally provides three-dimensional views of the defects within the tooth-supporting bone, which allows improved treatment planning.³

Unfortunately, CBCT cannot detect changes within the bone prior to inflammation-induced bone loss occurring. The current ionising-radiation-based modalities only allow the diagnosis of quantifiable (i.e., that already occurred) tissue losses.⁴ However, due to the accumulation of free water in the extracellular space of inflammation-affected bony areas, MRI can depict these early changes associated with periodontal inflammation, namely the resulting osseous oedema.⁵ Pulse sequences defined to characterise bone with fat suppression sequences (e.g., short-tau inversion recovery, “STIR”) were already cited as an essential method to improve the differentiation between healthy and pathologic tissues⁶, as demanded for the proper diagnosis of periodontal diseases.

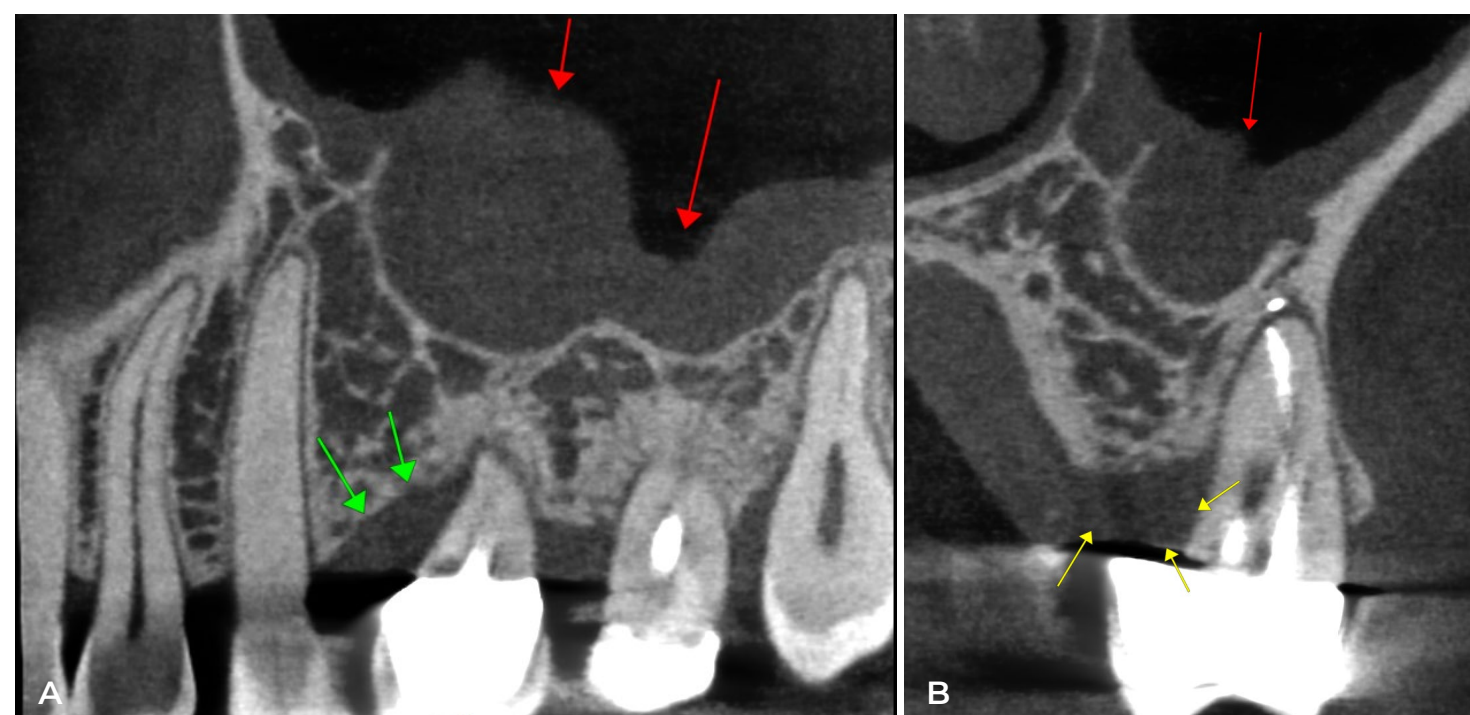


Fig. 12: CBCT of the left maxillary first molar, showing a well-defined bone loss extending through the three roots of the molar (yellow arrows in B), and angulated periodontal bone loss leading to the furcation involvement is seen (green arrows in A). There is visible thickening of the maxillary sinus membrane (red arrows in A and B).

In the following case, provided by Associate Professor Rubens Spin-Neto and co-workers, from Aarhus University, the patient (a 50-year-old female) presented to the clinics with a request for a CBCT to assist in defining the proper diagnosis and treatment plan regarding a furcation involvement (i.e., the loss of support bone in the area between the roots) of the left maxillary first molar. The tooth underwent root-canal treatment, but the periodontal status was still of concern. Therefore, the dentist wanted to assess the extension of bone loss and define the need for surgical intervention in the case. The CBCT (Fig. 12) shows bone loss extending through the three roots of the molar and angulated periodontal bone loss leading to the furcation. Due to the presence of root canal treatment and a prosthesis with metal, the CBCT image is rich in artefacts in the region-of-interest.

In the ddMRI (Fig. 13), the exam session included a scout-image (approximately 1 minute), followed by two separate PD-TSE slabs (approximately two-and-a-half minutes each), covering the sagittal and the coronal planes, and one sagittal PD-TSE-STIR slab (3 minutes) of the posterior maxillary region. The examination time was approximately 15 minutes, considering patient management time. The findings in the ddMRI agreed with those of the CBCT. ddMRI added information by suggesting a different type of soft tissue (i.e., not healthy dense gingiva) in the area of the furcation involvement, probably with some oedema associated with the area, as highlighted in the image acquired with STIR.

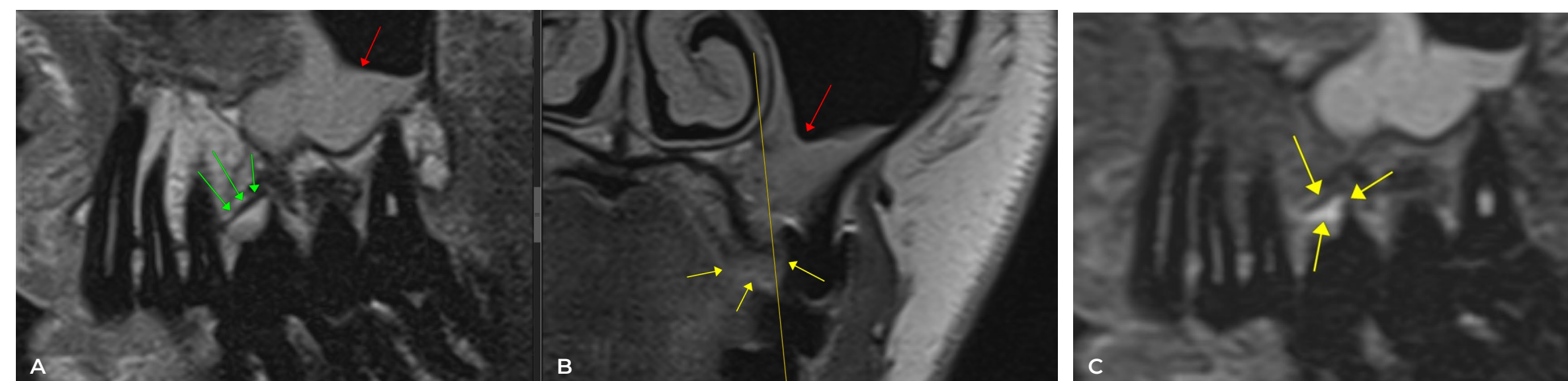


Fig. 13: ddMRI of the left maxillary first molar, showing bone loss extending through the three roots of the molar (yellow arrows in B), and angulated periodontal bone loss leading to the furcation involvement is seen (green arrows in A, yellow arrows in C). The images suggest oedema within the soft tissue between the roots (yellow arrows in C). There is visible thickening of the maxillary sinus membrane (red arrows in A, B, and C).

1 Kinane DF, Demuth DR, Gorr SU, Hajishengallis GN, Martin, MH. Human variability in innate immunity. *Periodontology* 2000. 2007, 45(1), 14–34. <https://doi.org/10.1111/j.1600-0757.2007.00220>.

2 Cimbaljevic MM, Spin-Neto RR, Miletic VJ, Jankovic SM, Aleksic ZM, Nikolic-Jakoba NS. Clinical and CBCT-based diagnosis of furcation involvement in patients with severe periodontitis. *Quintessence Int.* 2015 Nov-Dec;46(10):863-70. doi: 10.3290/j.qi.a34702.

3 Nikolic-Jakoba N, Spin-Neto R, Wenzel A. Cone-Beam Computed Tomography for Detection of Intrabony and Furcation Defects: A Systematic Review Based on a Hierarchical Model for Diagnostic Efficacy. *J Periodontol.* 2016 Jun;87(6):630-44. doi: 10.1902/jop.2016.150636.

4 Jergas M, Uffmann M, Escher H, Gluer CC, Young KC, Grampp S, Koster O, Genant HK: Interobserver variation in the detection of osteopenia by radiography and comparison with dual X-ray absorptiometry of the lumbar spine. *Skeletal Radiol.* 1994, 23 (3): 195-199.

5 Probst M, Burian E, Robl T, et al. Magnetic resonance imaging as a diagnostic tool for periodontal disease: A prospective study with correlation to standard clinical findings—Is there added value?. *J Clin Periodontol.* 2021;48:929–948. <https://doi.org/10.1111/jcpe.13458>.

6 Delfaut, E. M., Beltran, J., Johnson, G., Rousseau, J., Marchandise, X., & Cotten, A. (1999). Fat suppression in MR imaging: techniques and pitfalls. *Radiographics*, 19(2),373–382. <https://doi.org/10.1148/radiographics.19.2.g99m>.

Orthodontics

Treatment planning before orthodontic treatment often includes images such as lateral cephalograms, panoramas, and lately, CBCT volumes. These are used to annotate specific points, namely the “cephalometric” points, assess the patient’s soft-tissue profile, and provide an overview of the upper airways.¹ The cephalometric points help define the size, relative position, and angulation of the teeth and jaws, enabling the orthodontist to plan an appropriate and individualised treatment plan.² The craniofacial complex has been described using a variety of cephalometric methods. No particular analysis is thought to be better than another. In most examinations, the cranial base’s relatively stable components are used as reference points and measuring planes to gauge shifting or expanding structures. Similar images can be necessary during treatment for monitoring or after completion of the treatment for evaluation of the results and future reference.³

Most orthodontic treatments are performed on children or adolescents to utilise the patient’s growth potential and/or to prevent undesirable growth patterns’ effects. However, this patient group is more sensitive to ionising radiation than adults, with children having a radiation-effect multiplication factor of three, compared to the adult population.⁴ Considering the target patient population’s higher stochastic risk and the need for multiple images to be acquired during treatment, a non-ionising imaging modality would be preferable for orthodontic purposes. A single cephalogram is only one point in time, but a series of cephalograms over a few years gives the clinician valuable information on a patient’s growth tendencies. Realistic growth prediction requires at least two or three images to be acquired at 6-12 month intervals.

The choice modality must provide adequate coverage and image quality to allow proper diagnosis regarding the maxillary position, the mandibular position, facial proportions/vertical relationships, incisor positions (maxillary and mandibular), and the airway status. Some reference points, planes, and lines are “classic” and used across a variety of analyses.⁵

In the present case, provided by Associate Professor Rubens Spin-Neto and co-workers, from Aarhus University, ddMRI images of a volunteer (a 30-year-old female) were used to illustrate some of the most commonly used angles for cephalometric analysis. The exam session included a scout image (approximately 1 minute),

followed by one 3D acquisition using a PD-SPACE sequence, in a large field-of-view (i.e., full head), with an acquisition time of three-and-a-half minutes. The examination time was approximately 10 minutes, considering patient management time.

The image volume was used to generate a sagittal section, in which cephalometric points were annotated (Fig. 14): Sella (S, the centre of the hypophyseal fossa), Nasion (Na, the junction of the nasal and frontal bones at the most posterior point on the curvature of the bridge of the nose), “A-point” (A, an arbitrary measure point on the innermost curvature from the maxillary anterior nasal spine to the crest of the maxillary alveolar process, defining the most anterior point of the maxillary apical base), and “B-point” (B, an arbitrary measure point on the anterior bony curvature of the mandible, defining the innermost curvature from chin to alveolar junction). Relevant reference lines were also defined, those being the Sella-Nasion (S-N), Nasion-A point (Na-A), and Nasion-B point (Na-B). The angles among those lines are commonly used to define the relationship between the structures. In the present case, the horizontal relation between: the maxilla and the cranial base (the “SNA” angle, between the S-N and Na-A), the mandible and the cranial base (the “SNB” angle, between the S-N and Na-B), and the maxilla and the mandible (the “ANB” angle, represented by the SNA minus the SNB angles).

Using the same ddMRI-based sagittal section, the patient’s soft tissue and the airway profile were defined (i.e., traced). A panoramic reconstruction based on the ddMRI image volume was also generated as a way to provide further documentation on the case. It must be highlighted that the large field-of-view is placed to omit the brain tissues from the image, allowing the dentist to report on those anatomic structures within their field of expertise. The major advantage that ddMRI would provide in these orthodontic-related cases is that serial images during orthodontic treatment would be possible with increased patient safety, since no ionising-radiation-related risks are part of the process.



Fig. 14: ddMRI-based sagittal sections of a class I (i.e., healthy) patient. A shows the definition of the SNA angle, based on the S-N and Na-A reference lines. B shows the SNB angle, based on the S-N and Na-B reference lines. C shows the ANB angle, based on the previously mentioned angles.



Fig. 15: ddMRI-based sagittal sections of a class I (i.e., healthy) patient. In A, the patient’s soft tissue (red) and airway (green) profiles were traced. In B, a rendering of the soft tissues of the face is presented.

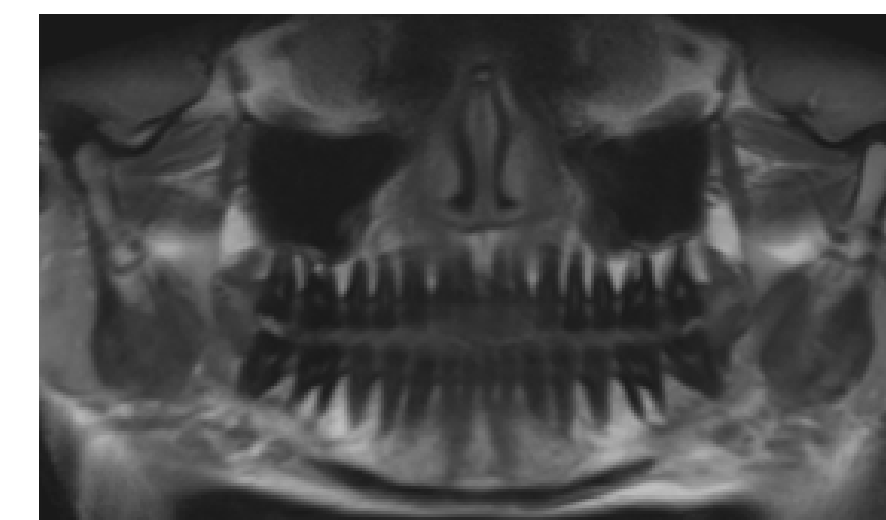


Fig. 16: ddMRI-based panoramic reconstruction, highlighting the TMJ area, the maxillary sinuses, the nasal cavity, and the upper and lower teeth.

- 1 Kapila SD, Nervina JM. CBCT in orthodontics: assessment of treatment outcomes and indications for its use. *Dentomaxillofac Radiol.* 2015;44(1):20140282. doi: 10.1259/dmfr.20140282.
- 2 Durão AR, Pittayapat P, Rockenbach MI, Olszewski R, Ng S, Ferreira AP, Jacobs R. Validity of 2D lateral cephalometry in orthodontics: a systematic review. *Prog Orthod.* 2013 Sep 20;14(1):31. doi: 10.1186/2196-1042-14-31.
- 3 da Silva MB, Sant’Anna EF. The evolution of cephalometric diagnosis in orthodontics. *Dental Press J Orthod.* 2013 May-Jun;18(3):63-71. doi: 10.1590/s2176-94512013000300011.
- 4 Oenning AC, Jacobs R, Salmon B; DIMITRA Research Group (<http://www.dimitra.be>). ALADAIP, beyond ALARA and towards personalized optimization for paediatric cone-beam CT. *Int J Paediatr Dent.* 2021 Sep;31(5):676-678. doi: 10.1111/ipd.12797.
- 5 Hurmerinta K, Rahkamo A, Haavikko K. Comparison between cephalometric classification methods for sagittal jaw relationships. *Eur J Oral Sci.* 1997 Jun;105(3):221-7. doi: 10.1111/j.1600-0722.1997.tb00204.x.

Temporomandibular Joint (TMJ) anatomy

MRI is already the accepted reference standard for diagnosis of temporomandibular joint disc displacement disorders,^{1,2} and for evaluation of TMJ inflammatory processes, such as those that occur in: juvenile idiopathic arthritis, synovitis, and in active severe degenerative joint disease.³ While imaging quality of MRI continues to improve, current medical MRI does not provide enough bony detail to sufficiently evaluate for bony pathologies in the TMJs.⁴

Clinicians, especially those managing orofacial pain, often use conventional MRI to evaluate these structures. However, obtaining these images can be cumbersome to both patients and clinicians. This occurs because dental providers rarely have MRI systems co-located at

their clinics. Even for providers affiliated with medical systems equipped with conventional MRI, obtaining access to schedule medical patients can be problematic let alone the feasibility of same-day scanning.

Here we present example images of healthy TMJs to demonstrate normal anatomy as it appears in ddMRI (Fig. 17 and Fig. 18). The CBCT images were provided by Prof. Donald Nixdorf, University of Minnesota. The ddMRI images were gently provided by Associate Prof. Rubens Spin-Neto, and co-workers, from Aarhus University. For comparison purposes, an annotated line drawing and a CBCT of a different healthy volunteer is provided to offer orientation. The examination session included a scout-image (approximately 1 minute), followed by

bilateral sets of paracoronal and parasagittal PD-TSE slabs (approximately three minutes each slab), with a field-of-view restricted to cover the TMJ area (70 x 70 mm). Additionally, bilateral parasagittal slabs using PD-STIR and T2 sequences were acquired (approximately three-and-a-half minutes each). The examination time was approximately 20 minutes, considering patient management time.

Key features to note include that the ddMRI clearly reveals the intraarticular disc interposed between the articular eminence and the condylar head in the closed-mouth position. Additionally, due to the fluid presence within the superior and inferior joint spaces, if inflammation were present, it would appear clearly as a

bright white signal. However, in the absence of disease as we show here, only a slight hyperintensity is noted in the joint spaces compared to surrounding tissues. Furthermore, fibers of the musculature are apparent, specifically the lateral pterygoid muscle as it attaches to the disc and condylar neck. The CBCT image is still considered the gold standard for bony diagnosis, such as that for degenerative joint disease, but it provides no soft-tissue information, while ddMRI also shows a clear cortical bony outline of the condylar head in black.

Coronal TMJ

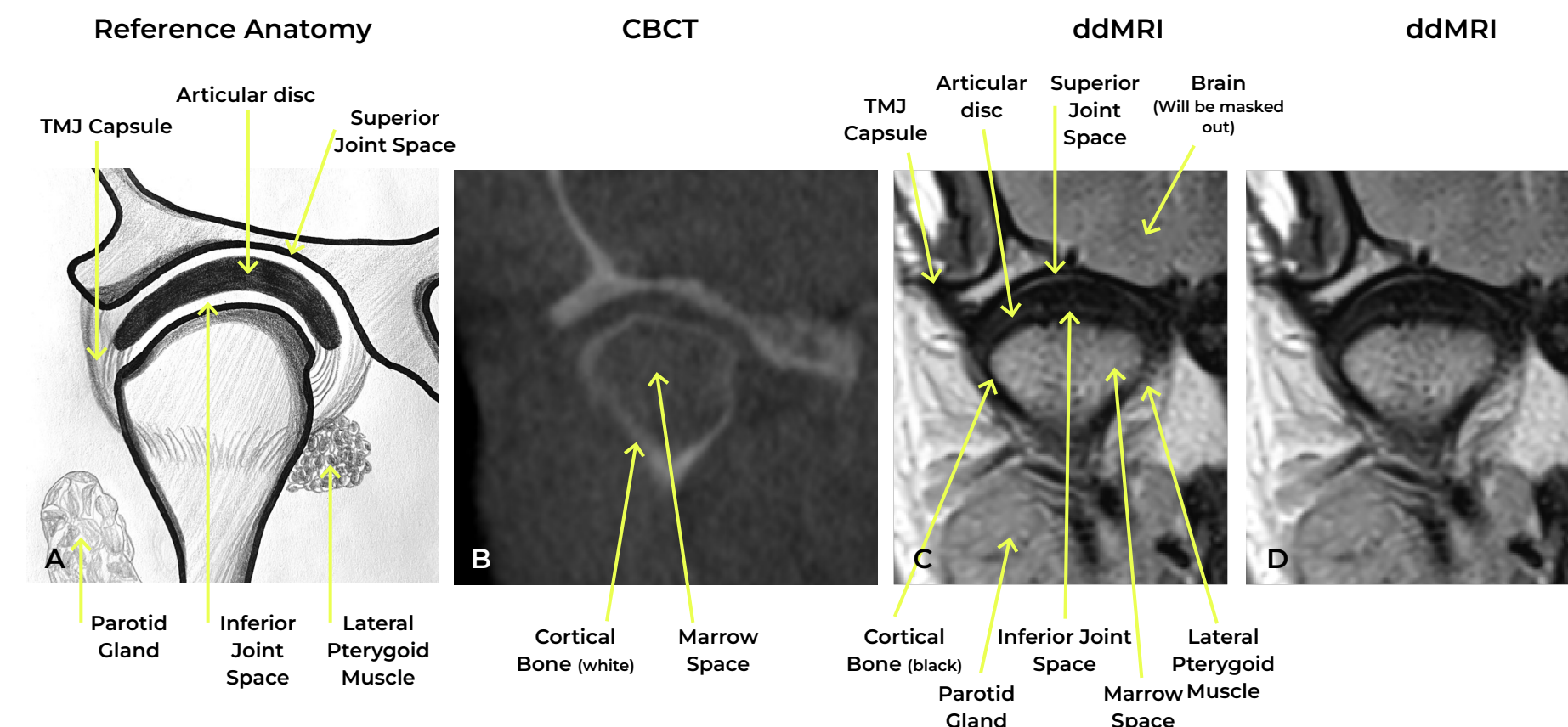


Fig. 17:
 A) Anatomical drawing of coronal section of TMJ
 B) CBCT of a TMJ from a healthy volunteer. Note no soft tissue information is available, but excellent bony resolution is present,
 C) ddMRI of a TMJ from a healthy volunteer with soft tissue features noted,
 D) Same ddMRI image from C), but without annotations for easier viewing.

Parasagittal TMJ

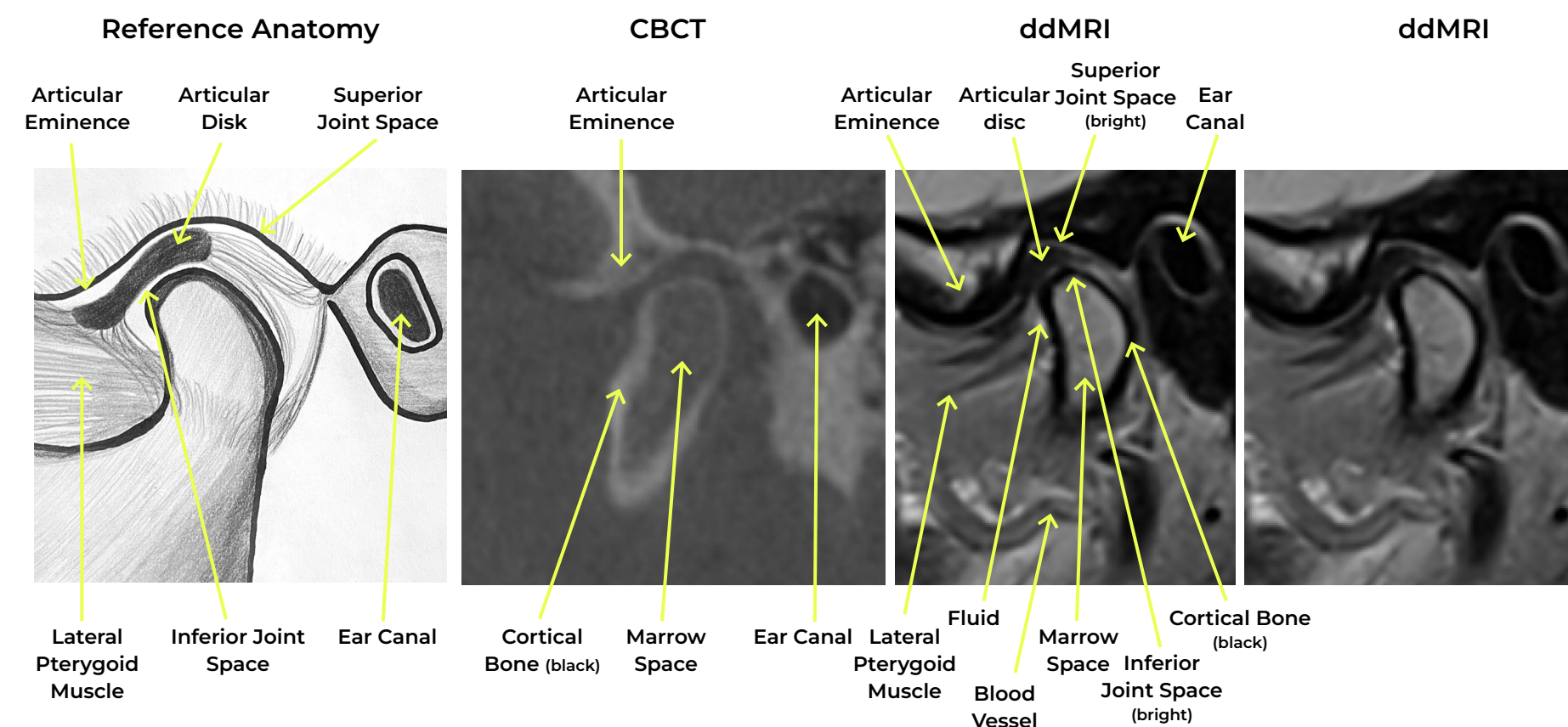


Fig. 18:
 A) Anatomical drawing of parasagittal section of TMJ
 B) CBCT of a TMJ from a healthy volunteer. Note no soft tissue information is available, but excellent bony resolution is present,
 C) ddMRI of a TMJ from a healthy volunteer with soft tissue features noted,
 D) same ddMRI image from C), but without annotations for easier viewing.

1 Ahmad M, Hollender L, Anderson Q, Kartha K, Ohrbach R, Truelove EL, John MT, Schiffman EL. Research diagnostic criteria for temporomandibular disorders (RDC/TMD): development of image analysis criteria and examiner reliability for image analysis. *Oral Surg Oral Med Oral Pathol Oral Radiol Endod.* 2009 Jun;107(6):844-60. doi: 10.1016/j.tripleo.2009.02.023. PMID: 19464658; PMCID: PMC3139469.
 2 Schiffman E, Ohrbach R, Truelove E, Look J, Anderson G, Goulet JP, List T, Svensson P, Gonzalez Y, Lobbezoo F, Michelotti A, Brooks SL, Ceusters W, Drangsholt M, Ettlin D, Gaul C, Goldberg LJ, Haythornthwaite JA, Hollender L, Jensen R, John MT, De Laat A, de Leeuw R, Maixner W, van der Meulen M, Murray GM, Nixdorf DR, Palla S, Petersson A, Pionchon P, Smith B, Visscher CM, Zakrzewska J, Dworkin SF; International RDC/TMD Consortium Network, International association for Dental Research; Orofacial Pain Special Interest Group, International Association for the Study of Pain. Diagnostic Criteria for Temporomandibular Disorders (DC/TMD) for Clinical and Research Applications: recommendations of the International RDC/TMD Consortium Network* and Orofacial Pain Special Interest Group†. *J Oral Facial Pain Headache.* 2014 Winter;28(1):6-27. doi: 10.11607/jop.1151. PMID: 24482784; PMCID: PMC4478082.
 3 Angeles-Han ST, Ringold S, Beukelman T, Lovell D, Cuello CA, Becker ML, Colbert RA, Feldman BM, Holland GN, Ferguson PJ, Gewanter H, Guzman J, Horonjeff J, Nigrovic PA, Ombrello MJ, Passo MH, Stoll ML, Rabinovich CE, Sen HN, Schneider R, Halyabar O, Hays K, Shah AA, Sullivan N, Szymanski AM, Turgunbaev M, Turner A, Reston J. 2019 American College of Rheumatology/Arthritis Foundation Guideline for the Screening, Monitoring, and Treatment of Juvenile Idiopathic Arthritis-Associated Uveitis. *Arthritis Rheumatol.* 2019 Jun;71(6):864-877. doi: 10.1002/art.40885. Epub 2019 Apr 25. PMID: 31021511; PMCID: PMC6788287.
 4 Kaimal S, Ahmad M, Kang W, Nixdorf D, Schiffman EL. Diagnostic accuracy of panoramic radiography and MRI for detecting signs of TMJ degenerative joint disease. *Gen Dent.* 2018 Jul-Aug;66(4):34-40. PMID: 29964246; PMCID: PMC9488601.



Outlook on Educational Concepts

KOL statements

“A ddMRI training course and timeline for the U.S. would include four tiers of training levels: OMF radiologists, general dentists/non-radiology specialists, training within dental schools, and specialty training in post-graduate programs. In the US and Canada specialist OMF radiologists already receive substantial training in foundational MRI knowledge and applications allowing an abbreviated course in terms of time. OMFR training would consist of details specific to the ddMRI unit including safety, clinical indications, image optimization, patient selection criteria, and interpretation of the images produced from the system. The technical training would be provided by the manufacturer and the rest by OMF radiologists trained as teachers specific to the ddMRI system and its images. A review of hard and soft tissue anatomy would be included. General dentistry and non-radiology specialists training would include the same topics covered in the OMF radiologist course but with an increased time commitment and emphasis on hands-on instruction. Such expanded training would be provided by the manufacturer and the specially trained OMF radiologists over a 4-5 day course. Training that takes place in dental schools including specialty training post graduate programs would have multiple components ideally distributed over 2-3 years of the program. The training components would include basic MRI physics and physical components, basic sequence physics and sequence selection, MR safety, patient selection criteria and image interpretation. The interpretation component would be ongoing throughout the entire clinical timeline of until graduation. Training for post-graduate programs would be similar to the dental school components, only compressed into a shorter time period. Instructional methods would include online material, lectures, videos and interactive sessions with ddMRI trained faculty with the highest emphasis on selection criteria and interpretation.”

“The possibilities and the limitations of MRI diagnostics in dentistry should already be taught in student teaching, especially in comparison with X-ray diagnostics. However, I see the more extensive discussion and the teaching of a specialist competence in dental MRI only after a dental professional experience of at least one year and ideally also after the acquisition of the CBCT specialist knowledge. Due to the then existing knowledge in the field of also three-dimensional imaging in dentistry, it will be possible, for example, to teach the indication, technical application and, above all, the reporting of MRI images of the dental, oral and maxillofacial region in a five-day course by specialists. This course could be supplemented by a compulsory independent reporting of a definable number of MRI images, to be reviewed by a specialist panel.”

“Inclusion of undergraduate teaching in ddMRI is essential, with an additional postgraduate training course basing on the former education. In undergraduate education, the basics of MRI should be taught to a level that a basic understanding of the technology is mandatory. Basing upon this undergraduate education, dedicated postgraduate ddMRI courses enable the more specific education in the dental application of the technology. For instance, such courses could be conducted as a one-week course with a strong emphasis on image interpretation, which is the most challenging part in MRI. Specialists in the field would train the participants on interpretation of existing ddMRIs. The course should also contain a supervised self-training plus a written interpretation of a certain number of ddMRI-images in the end of the course for each participant. Another major content of the course should be explanation of the different sequences that are implemented in the dedicated ddMRI-machines. Participants in the end of the course should be capable to select the appropriate sequence for a specific question. Plus, they should have acquired a basic knowledge on how to interpret ddMRI-images.”

“The ideal education timeline for ddMRI in Scandinavia should be aligned with that of CBCT. In Denmark, for example, five days of education are needed before a Dentist can work with CBCT images. Two days are technical-oriented, provided by the company selling the equipment, while a team of specialists in the field offers the last three days and covers the application part. In the first two days, attention is given to operating the unit and dealing with the patient workflow. For ddMRI, this would include the safety instructions and how to work at a magnetic field. As for the application part, this should be focused on topics that go from image quality optimization during acquisition to the proper indication of ddMRI and, most important, the interpretation of those images. Ideally, this will be done in a “diagnostic-task-oriented” manner, covering all aspects normally addressed by CBCT, but focusing on the added tissues that can now be reported on.”



USA

Prof. Dr. Donald Tyndall

President of the AAOMR, DDS, MSPH, PhD, FICD, Division of Diagnostic Sciences, Director Oral & Maxillofacial Radiology Predoctoral Program Section of Oral and Maxillofacial Radiology. The University of North Carolina at Chapel Hill



Germany

Prof. Dr. Dr. Stefan Haßfeld

Director Klinik für Mund-, Kiefer- und Gesichtschirurgie Plastische Operationen Lehrstuhl für Mund-, Kiefer- und Gesichtschirurgie an der Universität Witten/Herdecke



Switzerland

Prof. Dr. Ralf Schulze

Director Oral Diagnostic Sciences Clinic for Oral Surgery and Stomatology Bern University



Denmark

Assoc. Prof. Dr. Rubens Spin-Neto

Department of Dentistry and Oral Health Section for Oral Radiology Aarhus University



Discussion and Future Outlook

This whitepaper has aimed to provide initial evidence generated by leading dental experts to the decision-makers at universities, opening space for future cooperation within this new imaging modality realm.

The latest Global Oral Health Status Report published by the World Health Organization (WHO) shows that almost half of the world's population suffers from oral diseases.¹ The same report highlights that global cases of oral diseases have increased by 1 billion over the last 30 years, indicating that many people do not have access to the prevention and treatment of oral diseases. By developing new technologies that can be ultimately be used by a wide range of providers to detect diseases earlier, we are taking a big step toward making preventative healthcare more accessible. In agreement with that report, and even though MRI has become an indispensable diagnostic modality in medicine for diverse diagnoses and treatment planning², no dental-dedicated device has ever been provided by the healthcare and life sciences industries. It is time to invoke a change in this panorama and bring MRI into dentistry in a definitive manner through enabling ddMRI to come forward.

A paramount feature for research and educational institutions that wish to be established among the cutting-edge elite is to identify innovations with high potential to impact our daily practice as dentists. For example, the literature suggests that future research within dentomaxillofacial radiology should focus on further dose reduction or additional non-ionising imaging modalities (e.g., MRI)³ As the NIDCR Strategic plan for 2021-2026 highlights at this juncture, the compass is pointing towards a tailored, dental-

dedicated modality that can reach specialists, and ultimately general practitioners, and also satisfies clinicians and researchers alike in their quest for accurate diagnostic tools to improve the standard-of-care for dentistry.

The recently initiated clinical trials clarifying the possibilities of engaging ddMRI in the clinics are certainly the first of many steps to make this new modality accessible to all. The research possibilities are immense, and the claim for depending less on ionising radiation provides plausibility for more extensive multicentre studies and grant application consorts.

A group of leading dental experts is gathering the necessary evidence to set the stage for further clinical trials using ddMRI. In the coming two years, the goal is to make this new modality visible at specialised conferences and congresses in the field. The abstracts presented at these conferences and congresses will provide the basis for the first publications on the topic. Based on preliminary data, we anticipate these publications will provide evidence that ddMRI is not inferior to current state-of-the-art imaging modalities, while highlighting the added value of “making the invisible visible” for dentistry.⁴

The first publication on ddMRI can be found here:

Dentomaxillofacial Radiology, Volume 53, Issue 1, January 2024, Pages 74–85, [Dental-dedicated MRI, a novel approach for dentomaxillofacial diagnostic imaging: technical specifications and feasibility | Dentomaxillofacial Radiology | Oxford Academic](#)

1 Global oral health status report: towards universal health coverage for oral health by 2030. <https://www.who.int/publications/i/item/9789240061484> .

2 Yousaf T, Dervenoulas C, Politis M. Advances in MRI Methodology. Int Rev Neurobiol. 2018;141:31-76. doi: 10.1016/bs.irn.2018.08.008. Epub 2018 Sep 14. PMID: 30314602.

3 Bornstein MM. Current trends in dentomaxillofacial research - what is just hype, what has potential impact? Dentomaxillofac Radiol. 2021 Jul 1;50(5):20219004. doi: 10.1259/dmfr.20219004.

4 Idiyatullin D, Corum C, Moeller S, Prasad H, Garwood M, Nixdorf DR. Dental magnetic resonance imaging: making the invisible visible. J Endod. 2011 Jun;37(6):745-52. doi: 10.1016/j.joen.2011.02.022. Epub 2011 Apr 6.



Glossary

A

acquisition time (TA)

MR measurement: Measurement time for an entire data set. TA does not include the time needed for image reconstruction.

acquisition window

MR measurement: The time frame in a pulse sequence during which the MR signal is acquired.

active shielding (AS)

Magnetic field: For strong magnets, the [stray field](#) has to be actively shielded to increase the safety zone. For this purpose, secondary compensating coils are wound around the magnet, in opposite direction to the primary field-generating coils.

Gradients: Gradient systems with opposed coils used to reduce eddy currents.

active shim

Magnetic field: [Shimming](#) by adjusting the shim coil currents. Field inhomogeneity, which is partly disturbed by the patient, is improved.

aliasing artifact

Image quality: Overfolding artifacts are generated when the measured tissue is outside the FOV but still within the sensitive volume of the coil. Signals from outside the FOV overlap the image, but on the opposite side. Caused by the sampling and subsequent Fourier transform of signal components above the Nyquist frequency.

Remedied primarily through oversampling, but regional presaturation may be used as well.

array coil

MR components: An array coil combines the advantages of smaller coils (high signal-to-noise ratio) with those of larger coils (large field of view). It consists of multiple independent coil elements that can be combined depending on the requirements of the examination.

artifact

Image quality: Artifacts are signal intensities in an MR image that do not correspond to the spatial distribution of tissue in the image plane. They result mainly from physiological as well as system-related effects.

[> distortion artifact](#)

[> motion artifact](#)

AutoAlign (AA)

Slice positioning: Feature that facilitates the workflow for the preparation of an MR scan. The idea of AutoAlign is to assist the user in performing graphical slice positioning for MR examinations, mostly automated and with a reproducible precision in repeated scans, and scans for follow-up examinations. All MR applications, such as spine, neuro, muscular-skeletal, and cardiac imaging benefit from automatic slice positioning, however, the specific requirements differ between the anatomical regions. Each region may need a specific alignment algorithm. The names for these region-specific AutoAlign features are, for example, AutoAlign Knee, AutoAlign Spine, etc.

autocalibration

MR measurement: When using Parallel Acquisition Techniques (PAT), [coil profile](#) information, which is required for reconstruction, is obtained by a calibration measurement. Autocalibration is integrated in the measurement and is both faster (approx. 1 second) and in many cases more exact than a separate calibration. It is performed with sequence characteristics that are identical to those of the acquisition for the current patient position (including possible motions).

average

Measurement parameters: Average value of measured signals in a slice used to improve the signal-to-noise ratio (SNR). Averaging is performed, for example, on a measurement with 2 [acquisitions](#), that is, number of acquisitions (NA) = 2. The SNR increases with the root mean square of the number of averages.

B

bandwidth

Measurement parameters: Frequency range (minimum to maximum processed frequency) used for slice selection ([transmission bandwidth](#)) or image sampling (readout bandwidth).

The bandwidth describes which frequency range from the analyzed echo signal is transferred into one pixel (unit: Hz/pixel).

Increasing the bandwidth allows for shorter echo times and reduces the chemical shift artifacts. The disadvantage of a higher bandwidth is the larger amount of noise which is sampled due to larger frequency range. This translates into a lower signal-to-noise-ratio (SNR).

body coil

MR components: The body coil is an integral part of the magnet. It functions as a transceiver coil. It has a large measurement field, but does not have the high signal-to-noise ratio of dedicated coils.

B₀ field

MR physics: The static main magnetic field of a magnetic resonance system.

B₁ field

MR physics: The alternating magnetic field of RF radiation generated by a transmit coil.

C

coil

MR components: Antennas, called coils in the language of MR, are used to send RF pulses, or to receive MR signals, or both.

As transmit coils, they excite the nuclei in the volume of interest as homogeneously as possible, so that all nuclei receive the same level of excitation.

As receiver coils, they receive the MR signal with as little noise as possible. The signal strength depends among other things on the volume of excitation in the coil and the distance to the object to be measured. The noise, however, depends primarily on the size of the coil.

coil profile

MR physics: Receiver signal characteristics of an RF [coil](#), also known as coil sensitivity profile. The strength of the MR signal received from a voxel depends on the voxel location relative to the coil. In general, the signal is greatest in the vicinity of the coil. The further away the [voxel](#) is from the coil, the weaker the signal.

Coil profiles can be obtained either from a separate calibration measurement or by [autocalibration](#) integrated in the measurement.

contrast-to-noise ratio (CNR)

Image quality: The contrast-to-noise ratio in an MR image is the difference in the signal-to-noise ratios between two tissue types, A and B.

$$CNR = SNR_A - SNR_B$$

coronal plane

Slice orientation: Orthogonal plane dividing the body into back (dorsal, posterior) and front (ventral, anterior) parts.

cryogen

Magnet technology: Cooling agent such as liquid helium or nitrogen. In MR, cooling agents are used to maintain the superconductivity of the magnet.

curved planar reconstruction (CPR)

Postprocessing: CPR is similar to MPR, but can generate planar cross-sections through volume data that are orthogonal or tangential to a userdefined curve along an anatomic structure.



Glossary

D

data acquisition

MR measurement: Process of collecting raw image data from MR signals. To improve the [signal-to-noise ratio](#) in an image, several acquisitions can be performed to image a slice. Examples for data acquisition techniques: CISS, CAIPIRINHA, DESS, FISP, etc.

dedicated coil

> [local coil](#)

dephasing

MR physics: After RF excitation, phase differences appear between precessing spins, resulting in a decay of transverse magnetization.

Caused primarily by spin-spin interaction and inhomogeneity in the magnetic field, can also be caused by switching specific gradient fields (flow dephasing).

diamagnetism

MR physics: Effect resulting in a slightly weakened magnetic field when a substance is introduced into it. Magnetization of a diamagnetic material is opposite to the main magnetic field. The material is considered to have a negative magnetic [susceptibility \(magnetizability\)](#).

DICOM

Standard for electronic data exchange of medical images.

The DICOM standard enables the transfer of digital medical images and corresponding information, independent of device and manufacturer. In addition, DICOM provides an interface to hospital systems based on other standards.

distortion artifact

Image quality: Image distortions are caused by inhomogeneity in the magnetic field, gradient non-linearity, or ferromagnetic materials in proximity to the examination.

E

echo

MR physics: An echo is the refocusing of spin magnetization by a pulse of resonant electromagnetic radiation.

The MR signal observed following an initial excitation pulse decays with time due to both spin relaxation and any inhomogeneous effects which cause different spins in the sample to precess at different rates.

> [gradient echo \(GRE\)](#)

> [spin echo \(SE\)](#)

echo time (TE)

Measurement parameters: The time between the excitation pulse of a sequence and the resulting echo, which is used as MR signal. Determines image contrast.

excitation pulse

MRI measurement technique: Rotation of magnetization out of alignment with the longitudinal axis, caused by the application of an RF pulse. The higher the energy of an exciting RF pulse, the greater the deflection of the net magnetization. The deflection of the magnetization at the end of the RF pulse is known as the [flip angle](#).

F

fat saturation (FatSat)

Image quality: To suppress the fat component in the MR signal, fat protons are saturated by frequency-selective ("spectral") RF pulses. Fat saturation depends on the chemical shift between fat and water of approx. 3.5 ppm. Spectral fat saturation is sensitive to magnetic-field inhomogeneities.

fat suppression

Image quality: The MR signal comprises the sum of signals from water and fat protons. Various techniques can be used to suppress the fat signal.

> [STIR sequence](#)

ferromagnetism

Physics: Effect where a material, for example, iron, is drawn toward a magnetic field. Relevant to safety for MR imaging.

field of view (FOV)

Measurement parameters: Square image area to be measured (in mm × mm). For a fixed matrix size, the spatial resolution increases with a smaller field of view, because of smaller [voxels](#) (pixel size = FOV/matrix). However, smaller voxels yield lower signals.

field strength

> [magnetic field strength](#)

FLASH sequence

MRI measurement technique: The FLASH gradient-echo sequence uses the equilibrium of longitudinal magnetization. The remaining transverse magnetization is eliminated by a strong gradient (spoiler gradient). T1-weighted and T2*-weighted contrast can be set with the FLASH sequence.

flip angle

Measurement parameters: The flip angle α is used to define the angle of excitation for a pulse sequence.

It is the angle to which the net magnetization is rotated relative to the main magnetic field direction via the application of a RF excitation pulse at the Larmor frequency.

Flip angles between 0° and 90° are typically used in gradientecho sequences, 90° and a series of 180° pulses in spin-echo sequences and an initial 180° pulse followed by a 90° and a 180° pulse in inversion recovery sequences.

Fourier transform (FT)

Imaging: Mathematical procedure for reconstructing images from raw data. *MR spectroscopy:* Method for calculating MR spectra from time-resolved MRI data.

FOV

> [field of view \(FOV\)](#)

frequency

Physics: The number of repetitions of a periodic process per unit of time (unit: hertz).

fringe field

> [stray field](#)

G

Gauss

MR physics: Old unit for magnetic field strength. Today, the unit [Tesla \(T\)](#) is used (1 tesla = 10 000 gauss).

ghost image

Image quality: During movement such as breathing, some phase-encoding steps are acquired during inspiration (for example: inspiration phase), and others during expiration (for example: expiration phase). This quasi-periodic misencoding results in a displaced false image of the body region.

Signal-rich structures such as subcutaneous fat are particularly susceptible to ghost images due to movement. The distance between the ghost images depends on the movement period and relaxation time TR.

In echo-planar imaging, ghost images may occur at a distance of half the FOV.

gradient

MR physics: A gradient defines the strength and orientation of a magnitude changing in space. A magnetic field gradient is a change in the magnetic field of a certain orientation, a linear increase or decrease. The magnetic gradient fields are generated with [gradient coils](#).

They determine the spatial resolution in an image, for example.

gradient coil

MR components: Coils used to generate magnetic gradient fields. Gradient coils are operated in pairs in the magnet, at the same current, however, of opposite polarities.

One of the coils increases the static magnetic field by a certain amount, the opposite coil reduces it by the same amount.



Glossary

This changes the magnetic field overall. The change is the linear [gradient](#). According to the coordinate axes, there are x, y, and z gradient coils.

gradient echo (GRE)

MR physics: Echo created by switching a pair of dephasing and rephasing gradients, without a rephasing 180° pulse as with the spin-echo technique.

gradient field

> [gradient](#)

gradient strength

Gradient technology: Amplitude of the gradient field, measurement unit mT/m (millitesla per meter).

gradient system

MR components: In order to precisely localize the requested slice positions in MR imaging, the gradient system, consisting of three sets of gradient units (one for each direction), creates defined pulsed alterations of the main magnetic field, referred to as [gradients](#). For example, a whole-body gradient system is suitable for use in whole-body MR equipment.

H

head coil

MR components: Volume coil suitable for MRI examination of the patient's head.

head first

Positioning: The patient is positioned head first in the magnet bore.

head SAR

Safety: Specific absorption rate (SAR) averaged over the mass of the patient's head and over a specified time.

Hertz

Physics: SI unit of frequency (1 Hz = 1 s⁻¹).

homogeneity

Image quality: A magnetic field is considered homogeneous when it has the same field strength across the entire volume. With MR, the homogeneity of the static magnetic field is an important criterion for magnet quality. High homogeneity is important for spectral [fat saturation](#), a large [field of view \(FOV\)](#), off-center imaging, echo-planar imaging, and MR spectroscopy.

I

image contrast

Image quality: The contrast in the image is the relative difference in the signal strength between two adjacent tissue types.

It depends primarily on the existing tissue parameters ([T1](#), [T2](#), [proton density](#)), as well as flow, diffusion, etc.

Contrast can be affected by the sequence used ([spin echo](#), inversion recovery, [gradient echo](#), [TSE](#) etc.), the measurement parameters ([TR](#), [TE](#), [TI](#), [flip angle](#)) and the use of contrast agent.

image matrix

Image display: The MR image consists of a multitude of picture elements ([pixel](#)). Pixels are allocated to a matrix in a checkerboard pattern. Every pixel in the image matrix displays a specific gray scale level.

Viewed as a whole, the matrix of gray levels constitutes the image.

image noise

Image quality: Noise in the image is a statistical fluctuation in signal intensity that does not contribute to the image information. It appears in the image as a granular, irregular pattern. In principle, the effect is unavoidable and is physically based. The noise of the image is a function of the field strength, coil size (body coil, local coil, array coil), the pulse sequence used, and the spatial resolution.

image orientation

> [slice orientation](#)

image quality

The diagnostic quality of an MR image. Characteristics include:

> [artifact](#)

> [image contrast \(contrast-to-noise ratio\)](#)

> [image noise \(signal-to-noise ratio\)](#)

image reconstruction

The process of creating images from a set of [raw data](#) measured. With MRI, the [Fourier transform](#) is used for reconstruction.

imaging sequence

> [pulse sequence](#)

in-plane resolution

Image quality: In-plane resolution is determined by the size of the [pixels](#). The smaller the pixel, the better the in-plane resolution.

isocenter

Image quality: The main magnetic field is only [homogeneous](#) within a roughly spherical region about the isocenter of the magnetic field. In this area, the examination region is positioned to ensure the best possible image quality.

L

local coil

MR components: Local coils are RF receiver coils for individual parts of the body. Local coils have a high signal-to-noise ratio.

local SAR

Safety: Specific absorption rate (SAR) averaged over any 10 g of tissue of the patient's body and over a specified time.

localizer

Measurement: Image acquired as the basis for slice positioning. Synonym: scout.

longitudinal relaxation

MR physics: Return to equilibrium of the longitudinal magnetization after excitation, due to the energy exchange between the spins and surrounding lattice (also called spin-lattice relaxation).

longitudinal relaxation time

> [T1 constant \(longitudinal relaxation time\)](#)

M

magnet

A magnet is a material or object that produces a magnetic field. For details about specific types of magnets see:

> [permanent magnet](#)

> [resistive magnet](#)

> [superconductive magnet](#)

magnet bore

MR components: The magnet bore is the opening in the main magnet where the patient is placed for examination.

magnetic field

MR physics: The space surrounding a magnet (or a conductor with current flowing through it) has special characteristics. Every magnetic field exerts a force on magnetizable parts aligned along a primary axis (magnetic north or south pole). The effect and direction of this force is symbolized by magnetic field lines.

magnetic field gradient

> [gradient system](#)

> [stray field](#)

magnetic field homogeneity

> [homogeneity](#)

magnetic field strength

MR physics: The strength of the magnetic field force on magnetizable parts. In physics, the effect is called magnetic induction. In MR, it is referred to as magnetic field strength. Units: Tesla (T), 1 Tesla is approximately 20 000 times the strength of the earth's magnetic field.



Glossary

magnetic resonance (MR)

MR physics: Absorption or emission of electromagnetic energy by atomic nuclei in a static magnetic field, after excitation by electromagnetic RF radiation at [resonance frequency](#).

magnetic resonance imaging (MRI)

Images of objects, for example, the human body, are displayed with magnetic resonance using magnetic gradient fields. In practical application, the distribution of protons in the body is displayed.

The clinically relevant objective of MR imaging is the differentiation between pathological and healthy tissue ([image contrast](#)).

magnetization

MR physics: Magnetization is a quantity measuring the magnetic force a material can exert on its environment.

In MRI, the macroscopic magnetic net effect of [spin ensembles](#) is measured. This net magnetization of tissue [voxels](#) of interest determines the potential strength of the [MR signal](#).

matrix size

Measurement parameters: Size of the raw-data matrix; influences not only the spatial resolution, but also the measurement time and [signal-to-noise ratio](#).

With a square raw-data matrix, the number of rows equals the number of columns.

measurement field

Image quality: Spherical volume in the center of the magnetic field where the field has a defined homogeneity. For MRI examinations, objects to be measured have to be positioned at all times in the measurement field (to prevent signal distortions).

motion artifact

Image quality: Results from random or involuntary movement: breathing, heart-beat, blood flow, eye movement, swallowing, and patient movement. The effect appears as [ghost images](#) or smearing artifacts in the images. In the phase-encoding direction only.

MPRAGE

MRI measurement technique: MPRAGE is a 3D extension of the TurboFLASH technique with inversion preparation pulses. Only one segment or partition of a 3D data record is obtained per preparation pulse.

MR image

The MR image consists of a multitude of image elements, also known as [pixels](#). Pixels are allocated to a matrix in a checkered pattern. Every pixel in the image matrix displays a specific gray scale. Viewed as a whole, this gray scale matrix provides the image.

The gray scale of a pixel mirrors the measured signal intensity of the corresponding volume element ([voxel](#)). In turn, the signal intensity of a voxel depends on the respective transverse magnetization.

MR imaging

> [magnetic resonance imaging \(MRI\)](#)

MR signal

MR physics: Electromagnetic signal in the RF range. Caused by the precession of transverse magnetization created by a variable voltage in a receiver coil (dynamo principle).

The temporal progression of this voltage is the MR signal. Different MR signals in different tissue voxels generate the image contrast.

multiplanar reconstruction (MPR)

Postprocessing: Enables the calculation of images of any orientation to be reconstructed based on a 3D or gapless multi-slice measurement.

N

nuclear spin

MR physics: Atomic nuclei with an odd number of neutrons and protons have what is called nuclear spin. For MR imaging, mainly hydrogen protons are used. For MR spectroscopy, other nuclei are used as well, such as phosphorus, fluorine, and carbon.

number of slices

Measurement parameters: Multiple slices are usually acquired during an MR measurement. The maximum number of slices of a pulse sequence or measurement protocol depends on the repetition time TR.

P

partition thickness

3D imaging: The effective slice thickness of individual partitions in a 3D slab is the slab thickness divided by the number of partitions.

patient coordinate system

In syngo MR clinical images, the orientation is stated by a patient-related coordinate system.

This system indicates the direction from which a user is looking at the patient and how a slice is positioned.

Coordinate axes are feet to head, right to left, and anterior to posterior.

pixel

Image quality: Smallest picture element of a digital image.

To display the MR image, every pixel in the image matrix contains a specific gray value.

$\text{Pixel size} = \text{FOV} / \text{matrix size}$

pixel intensity

Image quality: The gray value assigned to pixels in the image data, depending on tissue and measurement parameters.

postprocessing

Image evaluation: MR images can be manipulated in various ways for evaluation, for example, image subtraction, averaging, rotation, inversion, [multiplanar reconstruction \(MPR\)](#), maximum intensity projection (MIP), etc.

precession

MR physics: Gyration of the rotation axis of a spinning body around another line intersecting it so as to describe a cone.

proton density

MR physics: Number of hydrogen protons per unit of volume (generally: spin density).

proton density weighting

Image quality: In a proton density-weighted MR image, contrast is affected primarily by the proton density of the tissue to be displayed. T1 and T2 effects are suppressed.

pulse sequence

MR measurement: Chronological order of RF pulses and gradient pulses used to excite the volume to be measured, generate the signal, and provide spatial encoding.

Typical pulse sequences: spin echo, gradient echo, TSE, Inversion Recovery, EPI, etc.



Glossary

R

radio frequency (RF)

MR physics: Portion of the electromagnetic spectrum in which electromagnetic waves can be generated by alternating current fed to an antenna. The RF pulses used in MRI are commonly in the 1–100 MHz range. Their primary effect on the human body is energy dissipation in the form of heat, usually on the surface of the body.

Energy absorption is an important value for establishing safety thresholds.

> [specific absorption rate \(SAR\)](#)

raw data

MR measurement: The MR measurement does not directly obtain the image. Instead, raw data are generated that are subsequently reconstructed into an image.

receiver coil

MR components: A local coil that receives signals.

Excitation is applied via the body coil, the measured signal is the patient-specific signal response.

relaxation

MR physics: Dynamic, physical process where a system returns from a state of imbalance to equilibrium.

> [longitudinal relaxation](#)

> [transverse relaxation](#)

relaxation rate R1, R2, R2*

MR physics: Reciprocals of the relaxation times, T1, T2, and T2*.

- R1: longitudinal relaxation rate (1/T1)
- R2: transverse relaxation rate (1/T2)
- R2*: apparent transverse relaxation rate (1/T2*)

Relaxation rates provide information about tissue microstructure. Application: quantitative MRI, for example, noninvasive measurement and imaging of liver iron concentrations.

repetition time (TR)

Measurement parameters: In general, the time between two excitation pulses. Within the TR interval, signals may be acquired with one or more echo times, or one or more phase encodings (depending on the measurement technique). TR is one of the measurement parameters that determines contrast. The acquisition time (TA) is directly proportional to TR.

resolution

> [spatial resolution](#)

> [temporal resolution](#)

resonance

Physics: Exchange of energy between two systems at a specific frequency. In musical instruments, for example, strings at the same pitch will resonate.

resonance frequency

MR physics: The frequency at which resonance occurs. In MR, this frequency is used for the RF pulse in order to affect the spin equilibrium, that is, it matches the Larmor frequency of the spins.

RF coil

> [coil](#)

RF energy

> [radio frequency \(RF\)](#)

RF pulse

> [excitation pulse](#)

RF shielding

Image quality: The radiofrequency pulses used in MR are in the radio frequency range. They have to be shielded for two reasons:

- external electromagnetic waves (for example, radios, electrical machines) would distort the measurement and generate image artifacts
- to avoid interference with other receivers, the RF signals of the system should not extend beyond the system

RF shielding is provided by installing the magnet and receiver coils in a Faraday cage (a space that cannot be penetrated by high-frequency waves). For that purpose, the magnet room is, for example, shielded with copper, and windows are covered with electrically conductive screens.

S

scan

MR measurement:

1. Acquiring one or several MR signals after a single excitation pulse
2. Acquiring a complete raw-data record

scout

> [localizer](#)

shim

Magnetic field: Correction of magnetic field inhomogeneities caused by the magnet itself, ferromagnetic

objects, or the patient's body. The basic shim usually involves the introduction of small iron pieces in the magnet.

The patient-related fine shim is software-controlled and performed using a shim coil.

> [active shim](#)

> [global shim](#)

> [interactive shim](#)

> [local shim](#)

> [3D shim](#)

signal-to-noise ratio (SNR)

Image quality: Relationship between the intensity of signal and noise. Ways to improve SNR include:

- increasing the number of [averages](#)
- increasing the measurement volume (although spatial resolution degrades)
- using special coils and [local coils](#)
- smaller [bandwidth](#)
- shorter [echo time](#)
- thicker slice

slab thickness

3D imaging: The slice thickness of a 3D slab.

slice

Measurement parameters: Thin, three-dimensional cuboid uniquely defined by slice position, FOV, and slice thickness. The center plane of the slice is the image plane.

slice distance

Measurement parameters: The separation between the center planes of two sequential slices or 3D slabs.

slice gap

Measurement parameters: The gap between the nearest edges of two adjacent slices. Slice thickness + slice gap = slice distance.

slice orientation

Measurement parameters: Orthogonal planes are available for use as the basic slice orientation:

- [sagittal](#)
- [coronal](#)
- [transverse](#)

An oblique or double-oblique slice is obtained by rotating the slice out of the basic orientation.

slice position

Measurement parameters: The position of the slice to be measured within the area under examination.

slice selection

MR measurement: To display an MR image of the human body, the slice desired has to be selectively excited. For orthogonal slices, a magnetic field gradient is applied perpendicular to the desired slice plane (slice-selection gradient). Oblique and double-oblique slices are excited by simultaneously applying 2 or 3 gradient fields.

slice thickness

Measurement parameters: The thickness set for the slice to be measured. The thicker the slice, the stronger the signal and the better the [signal-to-noise ratio](#). However, spatial resolution drops.

Combined with the number of slices, this parameter determines the extension of the measurement area in the slice-selection direction.

specific absorption rate (SAR)

Safety: The RF energy absorbed per time unit and per kilogram. Absorption of RF energy can result in warming of the body. Energy absorption is an important value for establishing safety thresholds.

Unauthorized high local concentrations of RF energy can result in burns (local SAR). When the RF energy is uniformly distributed, safety thresholds have to be observed to avoid, for example, cardiac stress (whole-body SAR).

Remedies: low-SAR RF pulses, smaller flip angles, lower TR, fewer slices.



Glossary

specific energy dose (SED)

Safety: The specific energy dose is the value of the accumulated whole-body SAR throughout the entire examination.

It is expressed in J/kg (= Ws/kg).

spin echo (SE)

MRI measurement technique: The reappearance of an MR signal after the decay of the FID signal. Dephasing of the spins (decay of transverse magnetization) is offset through the application of a 180° refocusing pulse. The spins rephase, producing the spin echo at time TE (echo time).

T2* effects (field inhomogeneity, susceptibility) are reversed but not T2 effects.

spin-echo sequence

MRI measurement technique: The sequence of an excitation pulse (90°) and refocusing pulse (180°) produces a [spin echo](#). Can be used to generate T1-weighted, proton-density-weighted or strong T2-weighted images.

spin ensemble

MR physics: Total of all spins in a volume element ([voxel](#)) creating the averaged macroscopic [magnetization](#) which yields the MR signal for this voxel.

spin-lattice relaxation

> [longitudinal relaxation](#)

spin-spin relaxation

> [transverse relaxation](#)

spin-spin relaxation time

> [T2 constant](#)
([transverse relaxation time](#))

STIR sequence

MRI measurement technique: Inversion recovery sequence with a short inversion time TI, used for [fat suppression](#).

TI selection depends on the field strength, for example, typical ranges are approx. 150 ms at 1.5 Tesla.

stray field

Safety: Magnetic field outside the magnet that does not contribute to imaging; also called fringe field. A specific distance has to be kept between the magnet and various devices and patients with cardiac pacemakers (for example: 0.5 mT line).

The stray field is low with permanent magnets because the system is largely self-shielding.

superconductive magnet

MR components: An electromagnet whose strong magnetic field (typically at least 0.5 T) is generated using superconductive coils. The conductive wires of the coils are made of a cryogenically cooled niobium titanium alloy, for example. Liquid helium is used as the cryogen.

superconductivity

Physics: Material characteristic of various alloys, which at very low temperatures (close to absolute zero) results in a complete loss of electrical resistance. Electrical current can then flow without loss, that is, the magnet is “always on” without any power supply.

surface coil

> [local coil](#)

susceptibility (magnetizability)

Physics: Measure for the ability of a material or tissue to be magnetized in an external magnetic field.

susceptibility artifact

Image quality: Local magnetic field gradients are produced in all transitions between tissues of differing magnetic susceptibility. In transitions between tissue and air-filled spaces (for example: the temporal bone), areas may be present that show reduced signal or no signal at all.

The effect is stronger with gradient-echo sequences, in particular EPI.

T

temporal resolution

Measurement parameters: Time duration between two acquisitions of the same region.

Tesla (T)

MR physics: SI unit for magnetic field strength. Approximately 20 000 times as strong as the earth's magnetic field (1 Tesla = 10 000 [Gauss](#)).

transceiver coil

MR components: A local coil that both sends and receives signals.

transmission bandwidth

MR measurement: The frequency range stimulated by the [excitation pulse](#) in a sequence.

transmit coil

MR components: A local coil that sends excitation pulses.

transverse relaxation

MR physics: Decay of transverse magnetization through the loss of phase coherence between precessing spins (due to spin exchange); is also known as spin-spin relaxation.

transverse relaxation time

> [T2 constant \(transverse relaxation time\)](#)

turbo spin echo (TurboSE, TSE)

MRI measurement technique: TSE is a fast multiecho sequence. Each echo of a pulse train receives a different phase encoding. Within one repetition time TR, raw-data rows equal to the number of pulse train echoes are acquired (segmented raw data).

The turbo factor increases speed, and is frequently used to improve resolution.

V

VIBE

MRI measurement technique: FLASH 3D imaging technique with reduced data acquisition time by using data interpolation, or partial Fourier techniques, or both, primarily for dynamic contrast-enhanced examinations of the abdomen.

voxel

Imaging: Volume element of the sample to be examined which is assigned to a pixel in the image matrix.

Voxel size = slice thickness × pixel size

3

3D imaging

MRI measurement technique: In 3D imaging, the entire measurement volume, the 3D slab, is excited and not just single slices. Additional phase encoding in the slice-selection direction provides information in this direction.

3D TSE

MRI measurement technique: As a 3D sequence, TSE allows for the acquisition of T2 images with thin slices and practically uniform voxels.

T1 constant (longitudinal relaxation time)

MR physics: Tissue-specific time constant which describes the return of the longitudinal magnetization to equilibrium. After time T1, the longitudinal magnetization grows back to approx. 63 % of its end value. A tissue parameter that determines contrast.

T1 contrast

Image quality: Since different types of tissue show different T1 relaxation, this difference can be shown as image contrast ([T1 weighting](#)).

Rule of thumb: T1 contrast = TR short (to maximize T1 contrast), TE short (to minimize T2 contrast).

T1 weighting

> [T1 contrast](#)

T2 constant (transverse relaxation time)

MR physics: Tissue-specific time constant that describes the decay of transverse magnetization in an ideal homogeneous magnetic field. After time T2, transverse magnetization has lost 63 % of its original value. A tissue parameter that determines contrast.

T2 contrast

Image quality: Since different tissue types show different T2 relaxation, these differences are shown as image contrast ([T2 weighting](#)).

Rule of thumb: T2 contrast = TR long (to minimize T1 contrast), TE long (to maximize T2 contrast).

T2 weighting

> [T2 contrast](#)



Dentsply Sirona

Sirona Dental Systems GmbH
Fabrikstraße 31, 64625 Bensheim, Deutschland
dentsplysirona.com

Subject to technical changes and errors in the text. Order No. M43-C197-01-7600, 0224.

Registered trademarks, trade names and logos are used. Even if these are not identified as such in the respective places, the corresponding legal provisions apply. Unless otherwise stated, all comparative statements in this document refer to a comparison of Dentsply Sirona products with each other.

Strategic
Partner

SIEMENS
Healthineers

 **Dentsply
Sirona**